

NUCLEAR STRUCTURE--EXPERIMENT

FIRST RESULTS FROM THE REACTION PRODUCT MASS SEPARATOR (RPMS)

J. Nolen, L. Harwood, M.S. Curtin, E. Ormand, S. Bricker, B. Sherrill, Z-Q Xie and B.A. Brown

MSU-84-629

Since the last annual report the construction of the RPMS has been completed and it has been used to separate and study several neutron rich light isotopes. This device was described in some detail at the Oak Ridge Conference on Instrumentation for Heavy Ion Nuclear Research¹. The mechanical layout of the RPMS is shown in Fig. 1.

In the first runs with the RPMS we concentrated on learning how to tune the device to achieve m/q focus at the focal plane. Fig 2 shows the focal plane detector set up which has been used so far. The detectors are positioned in the air just outside a vacuum window at the end of the beam tube at the tail of the RPMS. There are adjustable brass defining slits in front of a 2-dimensional position-sensitive gas proportional counter. Behind the gas counter is a $\Delta E-E$ silicon detector telescope for isotope identification. To tune the RPMS a 35 MeV/nucleon ^{14}N beam was stopped in a Be target and He, Li and Be fragments which penetrated the target were focused by the RPMS to the detector system.

Neutron rich light isotopes were produced by using a 30 MeV/nucleon $^{18}\text{O}^{5+}$ beam. Targets of both Be and Ta were tried and it was found

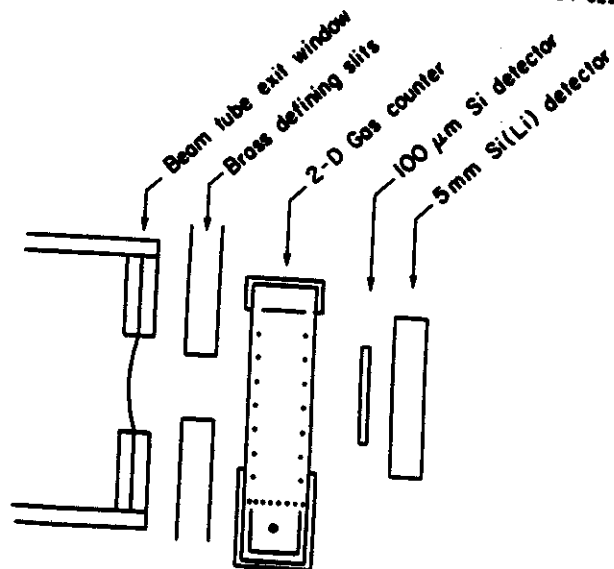


Fig. 2 Schematic drawing of the focal plane detector arrangement.

that the yield of neutron rich fragments was much greater from the Ta target. This is consistent with some preliminary results reported with the 40 MeV/nucleon argon beams at Ganil. Sample data with the RPMS tuned near $m/q=3$ and at low and medium dispersion are shown in Fig. 3. These data were recorded with the RPMS positioned at 0 degrees.

MSU-82-215

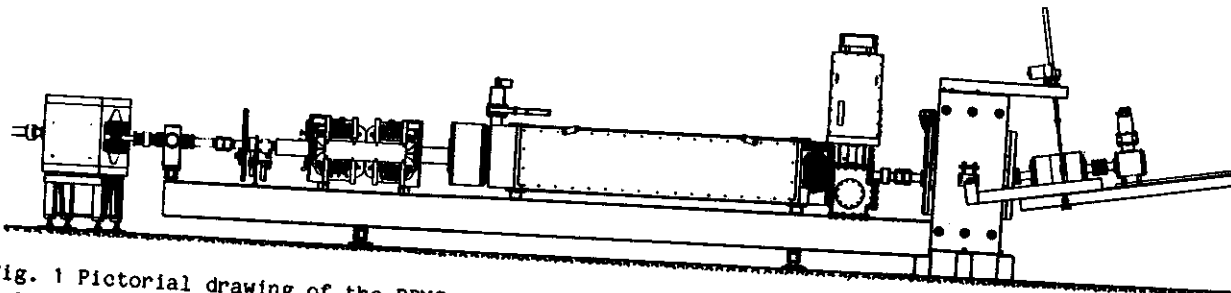


Fig. 1 Pictorial drawing of the RPMS. The beam inflector magnet is the first component at the left, followed by the bellows system and target chamber, aperture holder, quadrupole doublet, Wien filter (5m long) with high voltage supplies on the top right end, magnetic dipole and pivoting "tail" with quadrupole doublet and focal plane detectors at the right end.

J.S. Winfield, Sam M. Austin and Ziping Chen

Whether charge symmetry is broken in the nucleon-nucleon interaction has long been a problem of interest¹. Although nucleon-nucleon scattering experiments have become more precise and their interpretation less ambiguous, the present limits do not preclude that charge symmetry breaking (CSB) of the nuclear mean field might have significant effects on nuclear phenomena. Perhaps the best evidence for such effects is the Nolen-Schiffer or Coulomb energy anomaly². Negele concluded³ that the simplest explanation of the anomaly was that the single particle potential felt by a valence neutron is more attractive than that felt by a valence proton, by an amount corresponding to a volume integral difference of $19 \text{ MeV}\cdot\text{fm}^3$.

Another experimental phenomenon which may exhibit CSB is the difference in optical potentials for scattering of protons and neutrons from an $N=Z$ target. The accuracy of the potentials required (about 5%) is just feasible with state-of-the-art scattering data. Such a comparison has been done by DeVito et al.⁴ for the case of a ^{40}Ca target: after correcting for simple Coulomb effects, they found that the proton potential was slightly deeper than the neutron potential. Their result was almost three standard deviations removed from the CSB potential proposed by Negele to explain the Coulomb energy anomaly.

We have extended the work of DeVito et al. to targets of ^{32}S , ^{28}Si and ^{12}C . A difficulty with these nuclei is that they have strongly-excited collective states; therefore it seemed prudent to analyse the data within the coupled channels (CC) formalism. The inelastic channels included in the CCBA searches are listed in Table 1. Initial OM parameters for the searches were taken from the literature.

The general procedure followed that of Ref. 4 and is only summarised here. The volume integrals of the real optical potentials for

proton scattering are plotted against incident energy and a straight-line fit is made. This linear function is subtracted away from the real volume integrals found for the neutron scattering and the average of these differences, $(J_n - J_p)$, is found. It is necessary to correct this difference for the slowing down of the protons by Coulomb repulsion: because the (local) OMP is energy dependent, the protons thus feel a stronger nuclear attraction than do neutrons of the same incident energy. To determine this correction for ^{28}Si , we have carried out a computational experiment similar to that used by DeVito et al. for ^{40}Ca , whereby a series of proton scattering calculations with different energies are compared to a given neutron scattering case. The Coulomb shift, ΔE_c , is taken as the difference in energy which makes the diffraction maxima and minima fall at the same angle. The result for ^{28}Si was $\Delta E_c = 5.7 \pm 0.4 \text{ MeV}$. Combining this with the ^{40}Ca result, $\Delta E_c(^{40}\text{Ca}) = 7.0 \pm 0.6$, and assuming a functional form of $Z/A^{1/3}$, yields estimates of $\Delta E_c(^{32}\text{S}) = 6.1 \pm 0.6 \text{ MeV}$ and $\Delta E_c(^{12}\text{C}) = 3.2 \pm 0.4 \text{ MeV}$.

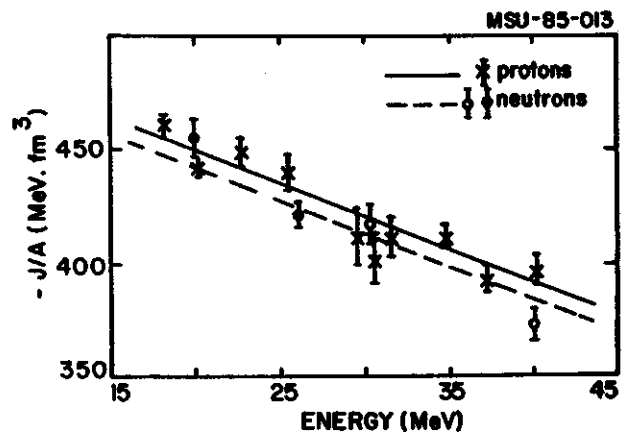


Fig. 1 Volume integrals per nucleon for proton and neutron scattering from ^{28}Si plotted against incident energy. Open circles, Ref. 9; solid circles, Ref. 10; crosses, Ref. 11. The lines are least-squares fits, assuming the same slope for neutrons as for protons.

A simple folding model is used to relate the difference between real OM potentials to the CSB potential of Negele (see Ref. 4 for details). We define

$$J^{CSB} = 2(J_n - J_p')/A$$

where J_p' is the volume integral for proton scattering corrected for the Coulomb shift.

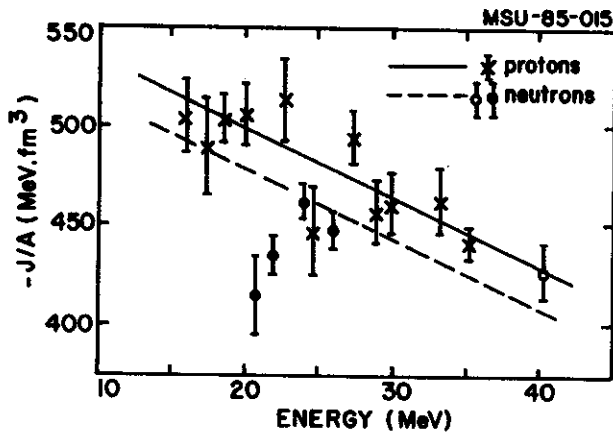


Fig. 2 Volume integrals per nucleon for proton and neutron scattering from ^{12}C plotted against incident energy. Open circles, Ref. 6; solid circles, Ref. 12; crosses, Ref. 13.

The values of J_n and J_p found for ^{28}Si , ^{12}C and ^{32}S are displayed in Figs. 1, 2 and 3, respectively. Results from the CC analysis by Taylor⁵ of nucleon scattering from ^{32}S have been supplemented by additional neutron data at 30.3 and 40.3 MeV from MSU⁶. Since the ^{28}Si CC analysis gave significantly different results compared to an earlier spherical OM analysis (see below), it was decided to repeat the work of DeVito et al. for ^{40}Ca (which was done with a spherical OM code) with the $3^-, 3.74$ MeV vibrational state now included explicitly. The CC analysis in this case did not significantly change J^{CSB} ($8 \pm 10 \text{ MeV}\cdot\text{fm}^3$, compared to $14 \pm 10 \text{ MeV}\cdot\text{fm}^3$ found by DeVito et al.).

As mentioned above, proton and neutron scattering from ^{28}Si showed different changes of the real potential when coupling was introduced (V_n increased in magnitude, V_p decreased). Although no complete explanation has been found for this, we have shown that at least part of the change is due to Coulomb excitation. The change is proportional to the square of the

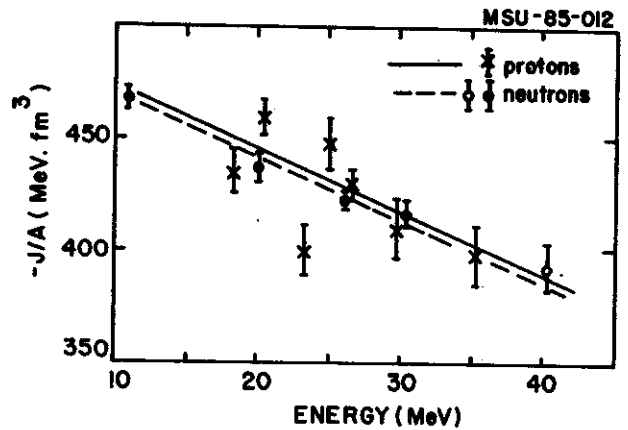


Fig. 3 Volume integrals per nucleon for proton and neutron scattering from ^{32}S plotted against incident energy. Open circles, Ref. 6; solid circles and crosses taken from Ref. 5.

coupling constant, which agrees with the findings of Perey⁷ for the case of proton scattering from ^{56}Fe .

Fig. 4 shows the differences in volume integrals for proton and neutron scattering for all four targets analysed here. The resulting values of J^{CSB} , as defined above, are given in Table 2.

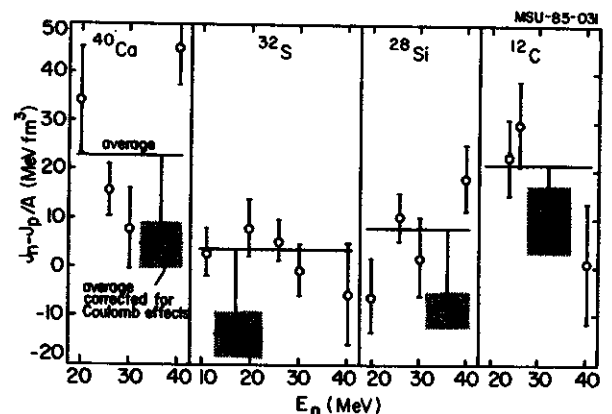


Fig. 4. Differences of proton and neutron volume integrals per nucleon for ^{40}Ca , ^{32}S , ^{28}Si and ^{12}C targets. The points are the differences between the fitted lines for protons (eg. from Fig. 1) and the data points for neutrons. The solid (dashed) lines are the averages before (after) correcting for Coulomb effects.

There are two corrections made to J^{CSB} in Table 2. The first concerns the Coulomb radius parameter used in the CCBA calculations. In order to avoid redoing all previous analyses,

most of these were done with a value taken from the OM parameter sets in the literature (typically $R_c = 1.2A^{1/3}$). With hindsight, one can see that values of R_c related to experimentally measured RMS charge radii of the target are preferable; these values were obtained from Ref. 8. Fortunately, the change in real potential depth for the associated changes in the Coulomb potential appears to be independent of the incident energy, so a correction to J_p/A (and thus to J^{CSB}) was estimated from sample cases rather than repeating all the original calculations.

The second correction in Table 2 arises because the proton and neutron distributions in the target nuclei are slightly different, with protons pushed to larger radii. Thus a measureable difference between proton and neutron scattering may be seen even if no CSB is present in the nucleon-nucleon force. Our estimate of this effect is taken from the difference in volume integrals of Hartree-Fock potentials for bound protons and neutrons, calculated with a charge-symmetric Skyrme interaction.

It is seen that the final values of J^{CSB} for the four targets are inconsistent (Table 2). To check whether the quoted uncertainties were realistic, some ^{28}Si calculations were repeated with alternative OM geometries. There was a systematic dependence of the individual volume integrals on geometry, but the difference $J_n - J_p$ agreed within errors. It should be noted that the uncertainties in the final J^{CSB} values do not include contributions from the corrections regarding the Coulomb radius and core polarization.

The ^{12}C result is probably the least reliable of the four: the lower energy $^{12}\text{C}(n,n)$ potentials were surprisingly less deep than those at 24 and 26 MeV (see Fig. 2), and in general the fits to the ^{12}C angular distributions were worse than those for the other targets. Perhaps the large deformation ($\beta_2 \approx 0.6$) has made the calculations inaccurate, or perhaps there are too few nucleons in ^{12}C for

such an "average" concept as the optical model to work at the required level of accuracy.

If the ^{12}C result is omitted, there still remains a marginal inconsistency between ^{40}Ca and the sd-shell nuclei. It appears that analyses in terms of standard phenomenological OMP's are subject to systematic uncertainties too large to permit a reliable determination of charge symmetry breaking effects in the mean field. Possible improvements might include the use of a folding model to determine the geometry of the real potential (the Woods-Saxon shape is not expected to be accurate for these light nuclei) or the use of model independent analyses as is done for electron scattering. It is clear that effects of core polarization must be included in some fashion, since its effects are comparable to any CSB effects.

Whether CSB in the nuclear mean field is a viable explanation of the Coulomb energy anomaly remains an open question. Our analysis for ^{40}Ca , including coupled channels effects, still yields a CSB potential inconsistent with this explanation at the two to three standard deviation level. As ^{40}Ca is the heaviest target studied and is subject to the smallest channel coupling effects, the ^{40}Ca result is perhaps the most reliable reported here. On the other hand, the results for the other targets certainly reduce one's confidence in the ^{40}Ca value. Indeed the mean for the three more reliable cases (^{40}Ca , ^{32}S and ^{28}Si) including the rough correction for core polarization, $-14 \pm 5 \text{ MeV fm}^3$, is consistent with the value of J^{CSB} proposed by Negele (-19 MeV fm^3) to account for the Coulomb energy anomaly.

Despite the marginal consistency, it does seem possible to use the present result to place limits on the magnitude of any CSB term in the mean field. Omitting the ^{12}C result, we set a "tight" limit (exclusive of uncertainties on each point) of

$$-24 \text{ MeV fm}^3 \leq J^{CSB} \leq 8 \text{ MeV fm}^3$$

and a "loose" limit (inclusive of the one standard deviation uncertainties) of

$$-33 \text{ MeV fm}^3 \leq J^{CSB} \leq 18 \text{ MeV fm}^3.$$

This work is now being written up as a paper.

Table 1 : Inelastic channels considered in the CCBA calculations.

Target	State	β_L
^{28}Si	2^+ , 1.78 MeV	-0.40
^{12}C	2^+ , 4.44 MeV	-0.60
^{32}S	2^+ , 2.23 MeV	+0.28
^{40}Ca	3^- , 3.74 MeV	+0.24

Table 2. Adjustments to J^{CSB} and final values (all in $\text{MeV}\cdot\text{fm}^3$).

Target	Coulomb radius ^a	Core polarization ^b	Final J^{CSB}
^{32}S	-6	+9	-24 ± 9
^{12}C	-8	+5	39 ± 13^c
^{28}Si	-11	+8	-21 ± 8
^{40}Ca	-10	+9	8 ± 10

a) Correction when Coulomb radius is taken from RMS charge radii

b) Estimate of change when core polarization is taken into account

c) From the fit to neutron data with $E_n > 21$ MeV. If the 20.8 MeV data is included, we obtain a final J^{CSB} of 45 ± 13 $\text{MeV}\cdot\text{fm}^3$.

1. For a recent review, see W. van Oers, Comments Nucl. Part. Phys. 10, 251 (1982)
2. J.A. Nolen, Jr. and J.P. Schiffer, Annu. Rev. Nucl. Sci. 19, 471 (1969)
3. J.W. Negele, Nucl. Phys. A165, 305 (1971)
4. R.P. DeVito et al., Phys. Rev. Lett. 47, 628 (1981)
5. R. Taylor, PhD. thesis, Ohio Univ. 1983 (unpublished)
6. R.P. DeVito, PhD. thesis, Michigan State Univ. 1979 (unpublished)
7. F.G. Perey, Phys. Rev. 131, 712 (1963)
8. B.A. Brown et al., J. Phys. G10, 1683 (1984)
9. R.P. DeVito et al., Phys. Rev. C 28, 2530 (1983)
10. J. Rapaport et al., Nucl. Phys. A286, 232 (1977)
11. R. De Leo et al., Phys. Rev. C 19, 646 (1979)
12. A.S. Meigooni et al., Phys. Med. Biol. 29, 643 (1984)
13. R. De Leo et al., Nucl. Phys. A254, 156 (1975)

MULTIPOLE MOMENTS OF ^{176}Yb AND ^{182}W FROM (\bar{p}, p') REACTIONS at 134 MeV.

B.G. Lay^a, S.M. Banks^a, B.M. Spicer^a, G.G. Shute^a, V.C. Officer^a, B.M. Ronningen, G.M. Crawley, N. Anantaraman and R.P. DeVito

We have completed the coupled channels analysis of the cross sections and asymmetries for the ground state rotational band members up to $J^\pi = 6^+$ in ^{176}Yb and ^{182}W , excited in (\bar{p}, p') reactions at 134 MeV. One goal of this and our similar study¹ of ^{154}Sm and ^{166}Er using the same reaction is to deduce the multipole moments of the matter distributions of these nuclei.

The best fits to these data are shown in Figs. 1 and 2. Using a theorem due to Satchler²

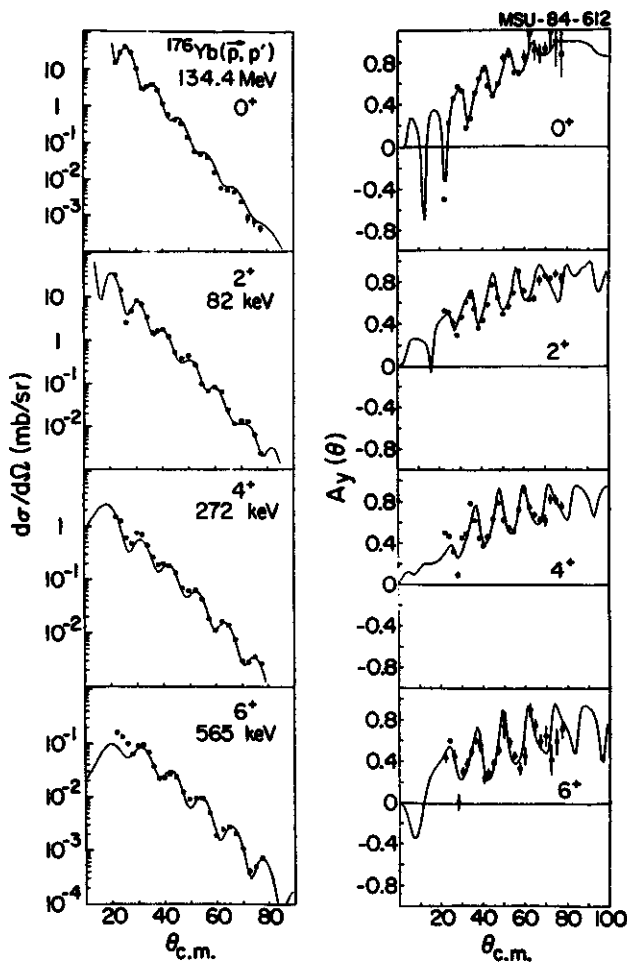


Fig. 1 Data for and coupled channels fits of differential cross sections and analyzing powers for excitation of ground state rotational band states to $J^\pi = 6^+$ in ^{176}Yb .

the normalized multipole moments of the deformed

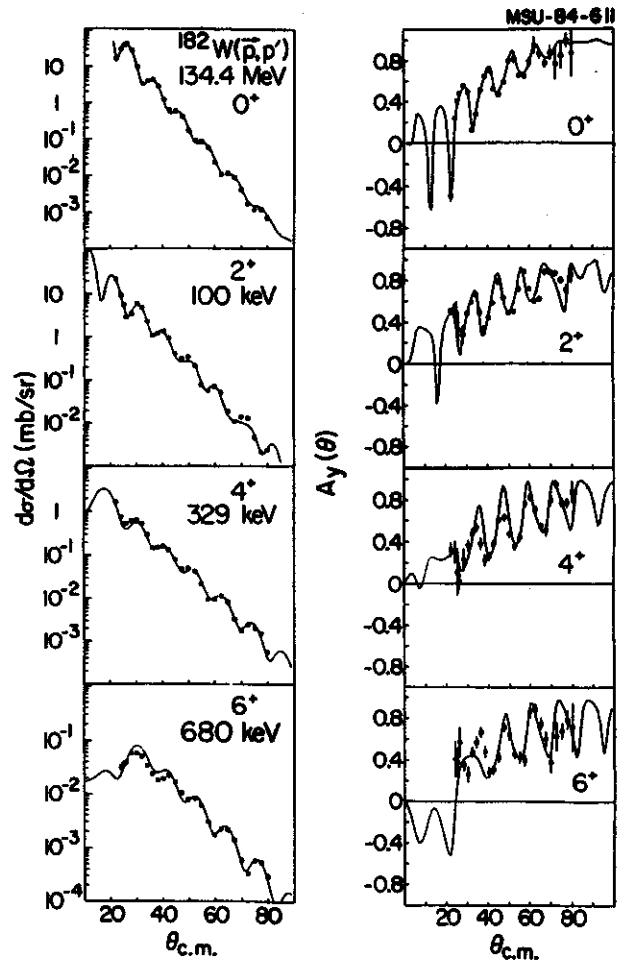


Fig. 2 Same as Fig. 1 but for ^{182}W .

optical model potential used to fit the data should be equal to the multipole moments of the matter distribution. This assumes that the potential is derivable from folding a central, scalar, energy and density independent interaction with the matter density. The multipole moments of the real part of the deformed optical model potential were calculated using the parameters from the best fits. These moments are given in Table 1.

The hexacontatetrapole deformation parameters from the present study, our previous study, and those from (α, α') and (p, p') reactions^{3,4,5} at other energies are shown in

Table 1. Multipole moments for ^{176}Yb and ^{182}W .

Nucleus	q_{20} (eb)	q_{40} (eb ²)	q_{60} (eb ³)
^{176}Yb	2.31(6)	-0.052(44)	-0.054(24)
^{182}W	2.03(6)	-0.25($\frac{13}{33}$)	-0.068($\frac{6}{14}$)

Fig. 3. Also shown are theoretical calculations by Nilsson et al.⁶ If our result for ^{154}Sm is correct the theoretically expected trend is verified for the first time.

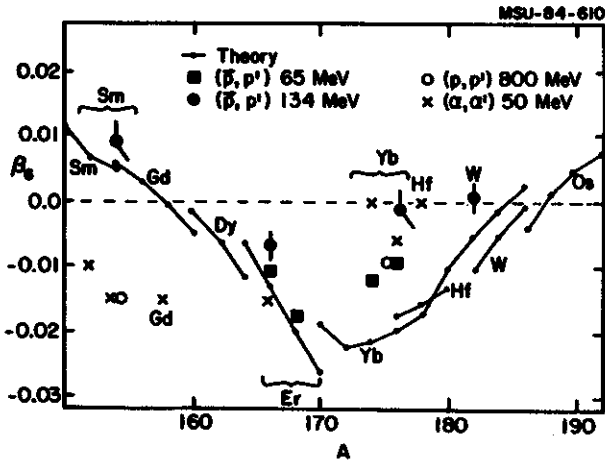


Fig. 3 Hexacontatetrapole deformation parameters in the rare earth region. The data from (α, α') and (p, p') reaction studies are from Ref. 3, 4, 1, and 5, respectively. The theoretical calculations are by Nilsson et al.⁶

a University of Melbourne, Parkville, Victoria 3052, Australia

b Indiana University Cyclotron Facility, Bloomington, Indiana 47405; Current address: Siemens Gammasonics Inc., 2000 Nuclear Drive, Des Plaines, Illinois 60018

1. R.M. Ronningen, G.M. Crawley, N. Anantaraman, S.M. Banks, B.M. Spicer, G.G. Shute, V.C. Officer, J.M.R. Wastell, D.W. Devins, and D.L. Friesel, Phys. Rev. C **28**, 123 (1983).

2. G.R. Satchler, J. Math. Phys. **13**, 1118 (1972).

3. D.L. Hendrie, N.K. Glendenning, B.G. Harvey, O.W. Jarvis, H.H. Duham, J. Saudinas, and J. Mahoney, Phys. Lett. **26B**, 127 (1968).

4. T. Ichihara, H. Sakaguchi, M. Nakamura, T. Noro, F. Ohtani, H. Sakamoto, H. Ogawa, M. Yosoi, M. Ieiri, N. Ishiki, and S. Kobayashi, Phys. Rev. C **29**, 1228 (1984).

5. M.L. Barlett, J.A. McGill, L. Ray, M.M. Barlett, G.W. Hoffmann, N.M. Hintz, G.S. Kyle, M.A. Franey, and G. Blanpied, Phys. Rev. C **22**, 1228 (1980).

6. S.G. Nilsson, Chin Fu Tsang, A Sobiczewski, Z. Szymanski, S. Wychech, C. Gustafson, I.-L. Lamm, P. Möller, and B. Nilsson, Nucl. Phys. **A131**, 1 (1969).

SPIN-FLIP TRANSITIONS WITH 201 MeV PROTONS.

G.M. Crawley, A. Galonsky, N. Anantaraman, G. Caskey, S.M. Austin^a, C. Djalali^b, N. Marty^b, M. Morlet^b, A. Willis^b and J-C. Jourdain^{*}.

High energy inelastic proton scattering is an excellent tool for studying $\lambda=0$ spin-flip transitions. The collaboration between MSU and Orsay used the facilities at the IPN, Orsay to study these transitions in a wide range of nuclei from ^{16}O to ^{208}Pb . In some cases in light nuclei, these transitions are to individual narrow levels but in most of the cases studied the level density is sufficiently high that the state appears as a broad bump. Much of this work has been presented in previous Annual Reports and has already been published. For example, the measurements on ^{208}Pb described briefly in last year's Annual Report will be published in the Physical Review in March 1985. In this report, we will discuss four current projects which are still either in the data taking or analysis stages and which have not yet been published or at least only preliminary or partial reports have been published.

1. The Nickel Isotopes studied by (p,p') and (p,n) Reactions.

Results of (p,p') measurements on the Ni isotopes ^{58}Ni , ^{60}Ni and ^{62}Ni were published in 1982¹⁾ as part of a general survey covering a wide range of nuclei. Since then further data have been taken on these isotopes and on the isotope ^{64}Ni . Preliminary results have been published²⁾ and a complete paper covering this work and making more complete comparisons with recent electron scattering measurements is presently in preparation. One very interesting feature of these data was the observation of the higher isospin component of the M1 transition.

Related measurements have also been carried out at the Indiana University Cyclotron laboratory of the (p,n) reaction on the same Ni isotopes. A paper on this work is about to be submitted. The various isospin components of

the analogous Gamow-Teller transitions were observed.

2. Ca Isotopes.

The results on ^{40}Ca have already been published³⁾ and those for the remaining Ca isotopes were summarised in the previous Annual Report (1982-83). A paper on all the Ca isotopes is almost complete.

There is quite good agreement between the (p,p') and (e,e') measurements on ^{40}Ca . However for ^{40}Ca , ^{42}Ca and ^{44}Ca , 1^+ states are observed in the (p,p') reaction where none are seen in (e,e') and vice-versa. Nor do the summed strengths agree. At least some of these differences are probably due to core excitations, including proton excitations in the lighter Ca isotopes.

3. s-d shell nuclei: ^{28}Si , ^{24}Mg , ^{26}Mg , ^{16}O , ^{18}O .

A paper describing the results on ^{28}Si has already been published⁴⁾ and a spectrum showing the T=0 and T=1 states is shown in Fig.1.

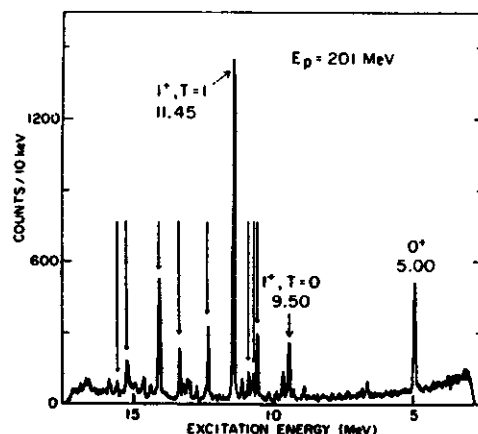


FIG. 1. Inelastic proton spectrum for ^{28}Si at 3.2° . The arrows indicate the one $T=0$ and nine $T=1$, 1^+ states observed.

Both $T=0$ and $T=1$, 1^+ excitations showed comparable quenching, the ratio of observed to

predicted strengths being about 30% for both isospins. In ^{24}Mg , it is again possible to separate transitions into primarily T=0 and T=1 on the basis of their angular distributions. The T=0 excitations have substantially flatter angular distributions. In contrast to the ^{28}Si case however, there appears to be little or no quenching in ^{24}Mg and in fact the experimental cross sections exceed the predicted values by about 20%. The data on ^{26}Mg is still being analysed.

Measurements have also been made on ^{16}O and ^{18}O using a gas target. While the quality of the data is not as good as from a solid target, 1^+ states were observed in both of these nuclei and angular distributions have been extracted between 2° and 7° . Fig.2 shows inelastic scattering cross sections plotted against center-of-mass angle for the known 16.22 MeV 1^+ state in ^{16}O . The cross section falls sharply beyond 5° . This strong forward peaking is characteristic of $l=0$ transitions. Further work is underway to obtain the absolute cross sections and to compare the data with shell model predictions using the DWBA formalism.

4. "Orbital" M1 Transitions.

The recent prediction⁵⁾ and subsequent observation⁶⁾ in (e,e') of low lying M1 transitions which are predominantly orbital in character, led us to search for similar states in (p,p') . Of course, if the character of the states is as predicted then we should not expect them to be strongly excited in (p,p') ⁷⁾. In fact the lack of observation of these transitions in (p,p') helps to confirm the orbital character of the transition. We have therefore carried out searches for these states in the heavy deformed nuclei ^{156}Gd , ^{152}Sm and ^{176}Dy but so far the low-lying 1^+ states seen in (e,e') have not been observed in the (p,p')

reaction.

Zamick⁸⁾ has pointed out, as has Brown⁹⁾, that similar states exist in lighter nuclei like ^{46}Ti and ^{48}Ti and we have also carried out a search in this mass region. Here the orbital character of the states is less pure. Our preliminary indications are that low lying 1^+ states are indeed observed in both ^{46}Ti and ^{48}Ti and comparisons will be made with electron scattering results to try to sort out the detailed structure of the states.

The (p,p') reaction has continued to prove a useful probe of $l=0$ spin-flip transitions and we have extended the range of our earlier measurements from light s-d shell nuclei to ^{208}Pb . Comparisons between (p,p') and (e,e') results for low lying transitions promises to give further insights into the structure of 1^+ states.

a Collaborated only on the Ni(p,n) reactions.
 b Institut de Physique Nucleaire, Orsay; collaborated on all (p,p') work but not on the Ni(p,n).

1. C. Djalali et al., Nuclear Physics A388, 1 (1982)
2. N. Marty et al., Nuclear Physics A396, 145c (1983)
3. G.M. Crawley et al., Physics Letters 127B, 322 (1983)
4. N. Anantaraman et al., Phys. Rev. Letters 52, 1409 (1984)
5. T. Suzuki and D.J. Rowe, Nucl. Phys. A289, 461 (1977); N. Loludice and B. Palumbo, Phys. Rev. Letters 41, 1532 (1978); Nucl. Phys. A326, 193 (1979); F. Iachello, Nucl. Phys. A358, 89c (1981); A.E.L. Dieperink, Prog. Part. Nucl. Phys. 9, 121 (1983)
6. D. Bohle et al., Physics Letters 137B, 27 (1984)
7. J.A. Carr et al., Phys. Rev. Letters 54, 881 (1985)
8. L. Zamick, preprint (1984)
9. B.A. Brown, private communication.

GIANT RESONANCES EXCITED WITH HIGH ENERGY LI SCATTERING

J. van der Plicht, W. Benenson, G. Crawley, E. Kashy, B. Sherrill, J.S. Winfield, H. Utsunomiya

An appreciable fraction of the information on nuclear giant resonances (GR) has been obtained with inelastic hadron scattering during the last decade - for the most recent review see ref. 1.

Most GR experiments were done with light ions, in particular alpha particles. In recent years, the field has been extended by using heavy ions as tools to investigate GR's - so far mainly results from inelastic scattering of ${}^6\text{Li}$, ${}^{12}\text{C}$, ${}^{14}\text{N}$ and ${}^{16}\text{O}$ at energies up to 20-25 MeV/nucleon have been reported.

In general, heavy ion inelastic scattering favors large L-transfers, and the background underneath the resonances may be smaller as compared to light ion scattering due to the absence of processes like knock-out and preequilibrium decay. On the other hand, heavy ion scattering is hampered by possible projectile excitations; also, the angular distributions are less sensitive to multipolarity as compared to light ions (see Ref. 2).

At our laboratory, we performed giant resonance experiments by inelastic scattering of ${}^6\text{Li}$ and ${}^{14}\text{N}$ at uniquely high beam energies of 35 MeV/nucleon. The ${}^{14}\text{N}$ data will be presented elsewhere in this annual report. We present here initial studies performed with ${}^6\text{Li}$ beams. For ${}^6\text{Li}$, experiments performed at 26 MeV/nucleon promised a very favourable resonance to background ratio. Also, for ${}^6\text{Li}$ inelastic scattering, projectile excitations are not serious at high energies because processes such as $({}^6\text{Li}, {}^7\text{Li} \rightarrow {}^6\text{Li} + n)$ appear at very high excitation energy ($E > 40$ MeV). We studied inelastic scattering of ${}^6\text{Li}$ at 35 MeV/nucleon on ${}^{58}\text{Ni}$, ${}^{90}\text{Zr}$ and ${}^{208}\text{Pb}$ targets. The experiment was performed using the S320 spectrograph. The angular range was 3-10 degrees (in the laboratory). Examples of $({}^6\text{Li}, {}^6\text{Li}')$ spectra are shown in Fig. 1. The Low Energy Octupole

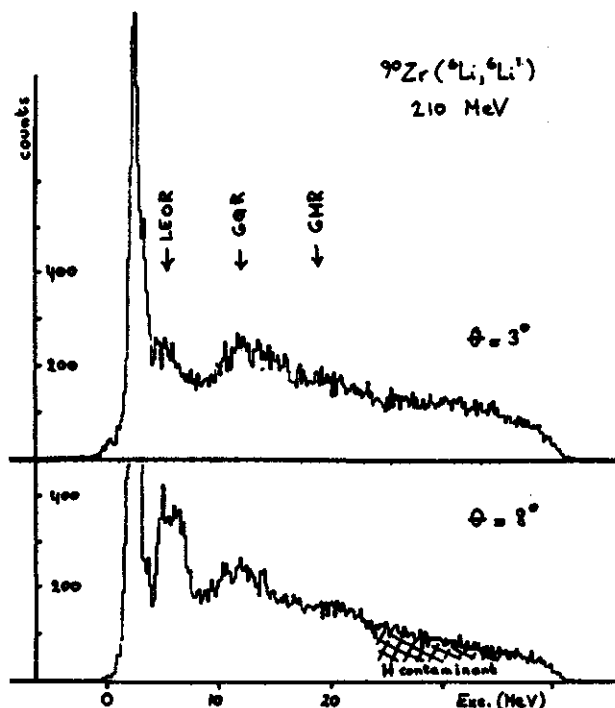


Fig. 1 ${}^{90}\text{Zr}$ Spectrum of inelastic scattering of ${}^6\text{Li}$ from ${}^{90}\text{Zr}$ measured at a beam energy of 35 MeV/nucleon.

Resonance (LEOR), Giant Monopole Resonance (GMR) and Giant Quadrupole Resonance (GQR) are clearly excited. The elastic peak was mostly blocked from the focal plane detector by a metal post; the sharp peak at the left of the spectrum is the tail.

The resonances observed are in agreement with other data (e.g. Ref. 5). However, the High Energy Octupole Resonance (HEOR), expected at around 25 MeV, is not observed. It appears that the resonance to background ratio is not much more favourable than found in light ion scattering.

Analysis of angular distributions is in progress. We plan to complete the data with inelastic scattering to low lying excited states (^{58}Ni), and elastic scattering in order to determine the optical potential (^{90}Zr).

1. J. Speth and A. van der Woude, Rep. Prog. Phys. 44,719(1981). 2. C.K. Gelbke, Giant Multipole Resonance Topical Conference, Oak Ridge 1979, proc. page 333. 3. U. Garg et al., this Annual Report. 4. H.J. Gils et al., Karlsruhe Annual Report, 1977, page 50. 5. T.P. Sjoreen et al., Phys. Rev. C 29,1370(1984).

EXPLORATORY STUDY OF GAMOW-TELLER TRANSITIONS WITH (${}^6\text{Li}, {}^6\text{He}$) AT 210 MeV

N. Anantaraman, J.S. Winfield, S.M. Austin, Z.P. Chen, A. Galonsky, J. van der Plicht, H.L. Wu, C.C. Chang^a, S.Gales^b and G.C. Ciangaru^c

We have studied the (${}^6\text{Li}, {}^6\text{He}$) reaction on targets of ${}^7\text{Li}$, ${}^{12}\text{C}$, ${}^{14}\text{C}$, ${}^{26}\text{Mg}$ and ${}^{90}\text{Zr}$ at a bombarding energy of 35 MeV/nucleon. The main objective was to investigate whether the reaction mechanism consists predominantly of the one-step process, so that cross sections at forward angles for $\Delta L=0$, $\Delta S=1$, $\Delta T=1$ (Gamow-Teller) transitions are a measure of Gamow-Teller (GT) strength. The targets used provided several well-resolved transitions for this purpose, with GT strengths known either from β -decay or from (p,n) studies. A similar calibration of (p,n) cross sections in terms of β -decay matrix elements proved¹⁾ to be very useful in extending the range of measured $B(\text{GT})$ values. Charge-exchange studies have previously been performed on all the targets used with intermediate-energy (p,n) reactions and in some cases with (${}^3\text{He}, t$) or lower energy (${}^6\text{Li}, {}^6\text{He}$) reactions.

Measurements were carried out with the S-320 spectrograph. The most complete set of data, including a measurement at 0° , was taken for the case of ${}^{14}\text{C}$. Spectra measured at 3.5° are shown in Fig. 1. The resolution was about 450 keV, which was adequate to resolve most of the low-lying 1^+ levels of interest: the ground states of ${}^{12}\text{N}$ and ${}^{14}\text{N}$, the strongly excited 3.95-MeV level of ${}^{14}\text{N}$ and the 1.06-MeV level of ${}^{26}\text{Al}$. The ground state ($3/2^-$) and the 0.43-MeV ($1/2^-$) state of ${}^7\text{Be}$, both of which are populated purely by GT transitions in our reaction, were not resolved, but a peak-fitting program enabled us to decompose the doublet. In ${}^{26}\text{Al}$, two 1^+ levels at 1.85 and 2.07 MeV were unresolved, and were treated as a doublet in the analysis. The peak at 2.3 MeV in ${}^{90}\text{Nb}$ was taken to correspond to the peak at the same excitation energy seen in the (p,n) reaction at 120 MeV²⁾, where it has been identified as a cluster of 1^+ levels.

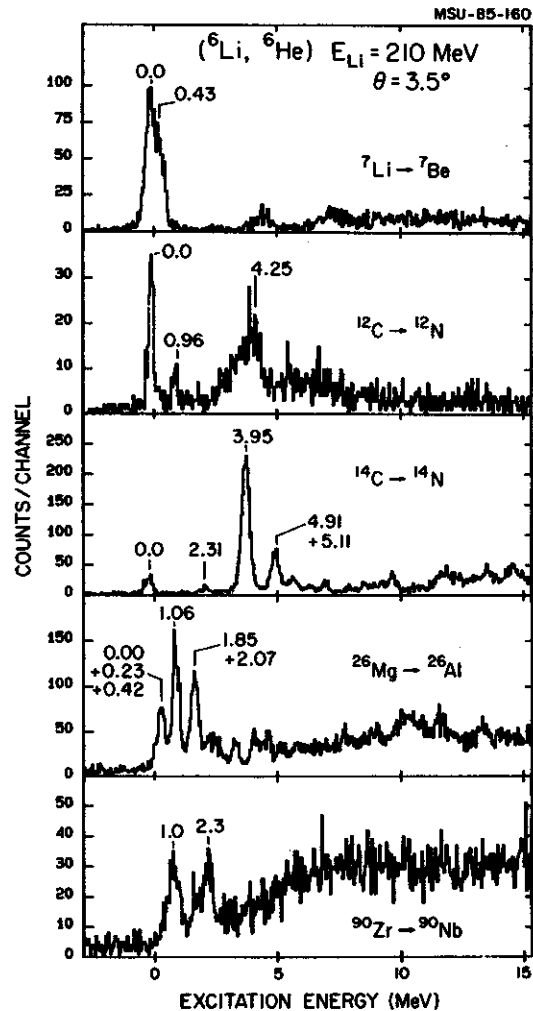


Fig. 1 Spectra measured at $\theta_{\text{lab}} = 3.5^\circ$ for the (${}^6\text{Li}, {}^6\text{He}$) reaction at 210 MeV on targets of ${}^7\text{Li}$, ${}^{12}\text{C}$, ${}^{14}\text{C}$, ${}^{26}\text{Mg}$ and ${}^{90}\text{Zr}$.

The investigation of the one-step nature of the reaction mechanism can be done at several levels. The simplest one is to compare the ratio of cross sections for the 0.0- and 0.43-MeV levels of ${}^7\text{Be}$ with the ratio of $B(\text{GT})$ values known from β -decay. Such a comparison avoids both the uncertainty of absolute cross section determinations and the need to correct for

distortion effects. We measured ${}^7\text{Li} \rightarrow {}^7\text{Be}$ cross sections at five angles from 2.5° to 6.5° . The ratio of cross sections, $\sigma(0.0)/\sigma(0.43)$, is 1.55 ± 0.16 at all angles except 2.5° , where it is 1.07 ± 0.11 . The corresponding B(GT) ratio is 1.18. The effect of tensor and exchange terms, present in the reaction but absent in the β -decay, may be responsible for the differences; this remains to be studied.

A second check on the one-step mechanism is the extent to which the angular distributions for the various GT transitions, when converted to plots of cross sections vs. momentum transfer, have the same shape and magnitudes proportional to B(GT) values. The shape comparison is made in Fig. 2, where all the cross sections are normalized to that for the ${}^{14}\text{N}(3.95 \text{ MeV})$ level at $q=100 \text{ MeV/c}$. With the exception of the two ${}^7\text{Be}$ curves, the shapes are all roughly the same. Fig. 3 shows that the magnitudes of the cross sections at a fixed momentum transfer (100 MeV/c) are roughly proportional to the known B(GT) values for the four light targets. The discrepancy in the case of ${}^{90}\text{Zr}$ may be partly due to the mass dependence of distortion effects; this is also the only case where the value of B(GT) is taken from (p,n) rather than β -decay studies.

A third check is to consider the relative populations of the 0.0, 2.31 and 3.95 MeV levels of ${}^{14}\text{N}$. The first two should not be seen at all, or seen only weakly, in the one-step process. From β -decay studies the ground state is known to have a B(GT) only about 10^{-5} of that for the 3.95-MeV level, but in the (p,n) reaction the ratio of cross sections is found to be 10^{-2} . In our measurement, the ratio is 0.1. The differences are presumably due to the effects of the tensor and exchange terms in the interaction or to L=2 amplitudes. Similarly, the 0^+ isobaric analogue state (IAS) at 2.31 MeV cannot be populated in our reaction except by the exchange term (in addition to possible two-step processes). The data show that the IAS has a cross section less than 0.1 of that of the

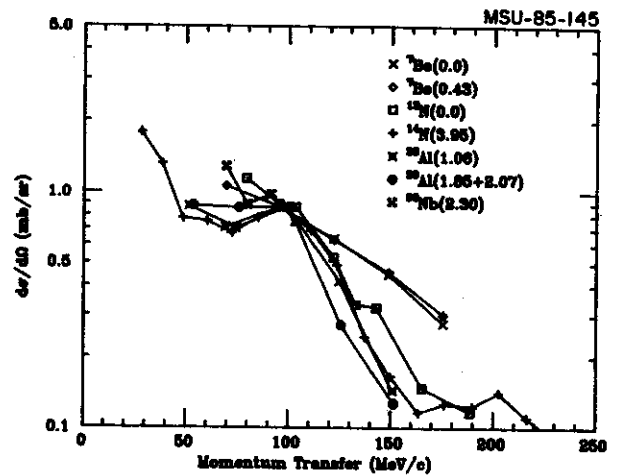


Fig. 2. Momentum transfer distributions for transitions to the levels indicated in the plot. All cross sections have been normalized to those for the ${}^{14}\text{N}(3.95 \text{ MeV})$ level. The lines are drawn to connect the data points.

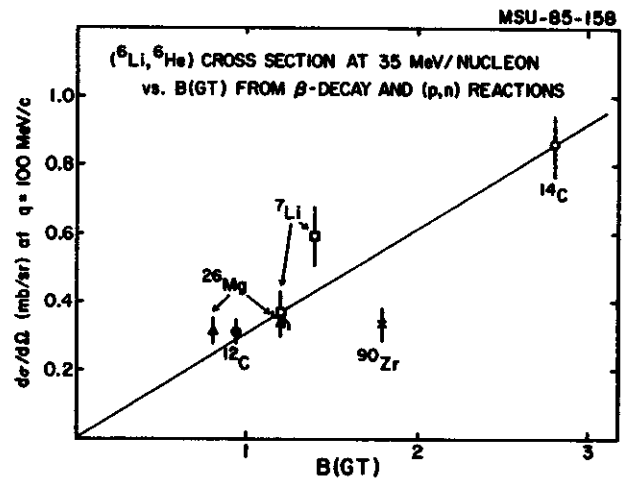


Fig. 3 Plot of $({}^6\text{Li}, {}^6\text{He})$ cross sections at 210 MeV for a momentum transfer of 100 MeV/c vs. B(GT) values.

3.95-MeV level and has a distinctive minimum (Fig. 4). At 35 MeV/nucleon, the ground state and the IAS are suppressed by a factor of 2 compared with the results³⁾ at 10 MeV/nucleon.

As a final check, we have begun to compare the cross sections for the ${}^{14}\text{N}$ levels with microscopic distorted-wave Born approximation calculations. Figure 4 shows the preliminary results of several one-step calculations, each

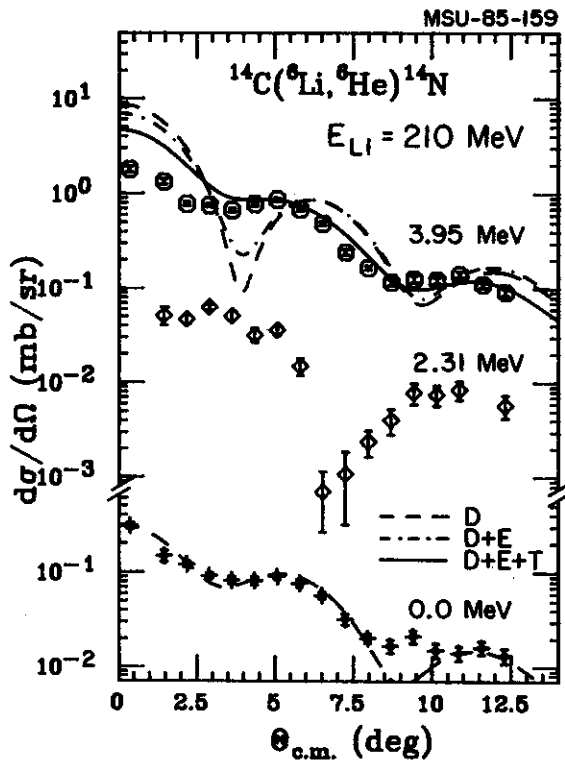


Fig. 4 Angular distributions for the $^{14}\text{C}(^6\text{Li}, ^6\text{He})^{14}\text{N}$ reaction at 210 MeV to the 3.95, 2.31 and 0.0 MeV levels of ^{14}N . The curves are calculations described in the text.

separately normalized to the data. Since optical-model potentials for ^6Li at 210 MeV are not yet available, potentials obtained⁴⁾ from 150-MeV data were used. Shell-model wave functions obtained with an interaction due to Millener⁵⁾ were used for the target and final nuclear states. Curves labelled D, D+E and D+E+T are respectively the results of including the direct, direct + exchange and direct + exchange + tensor terms, where the direct part corresponds to the $V_{\sigma\tau}$ part of the nucleon-nucleon interaction. The D calculations were done with the code SESIME⁶⁾ and the others with a modified form of DWUCK⁷⁾. The tensor term is needed to bring the calculation into phase with

the data at angles larger than 2.5° , but there is still room for improvement at smaller angles. (The exchange part of the tensor amplitude was not included in the calculation.) The normalizations obtained for the three calculations for the 3.95-MeV level, with a Yukawa interaction of 1-fm range and with the Millener wave functions renormalized to give the experimental B(GT) value, correspond to $V_{\sigma\tau}$ values comparable to the value of $11.7 \pm 1.7 \text{ MeV}$ obtained from (p,n) studies in this energy/nucleon range.

In summary, we have studied several GT transitions and find a correspondence between ($^6\text{Li}, ^6\text{He}$) cross sections at 210 MeV at forward angles and the known GT strengths. From this we conclude that the one-step process dominates the reaction mechanism. However, the energy resolution so far obtained at 210 MeV precludes the study of several interesting problems in spin-transfer physics. In a more recent study, we have obtained better resolution at 150 MeV; these data are presently being analyzed.

a University of Maryland, College Park, Maryland

b Institut de Physique Nucleaire, Orsay, France

c Schlumberger Well Services, Texas

1. C.D. Goodman et al., Phys. Rev. Lett. 44, 1755(1980).
2. D.E. Bainum et al., Phys. Rev. Lett. 44, 1751 (1980).
3. C.D. Goodman et al., Phys. Lett. 64B, 417 (1976); and W.R. Wharton et al., Phys. Rev. C22, 1138(1980).
4. J. Cook, Nucl. Phys. A388, 153(1982).
5. D. J. Millener, private communication.
6. A. Etchegoyen et al., Nucl. Phys. A397, 343 (1983).
7. G. Ciangaru et al., Nucl. Phys. A380, 147 (1982).

J.S. Winfield, N. Anantaraman, Sam M. Austin, L.H. Harwood, J. van der Plicht, H.-L. Wu
and A.F. Zeller

There have been only a few studies of charge-exchange reactions with projectiles heavier than lithium and most of these have been at energies less than 10 MeV/nucleon^{1,2}. At these energies, sequential transfer of nucleons dominates the simpler one-step mechanism associated with pion exchange. One expects the situation to reverse at higher energies since the sequential transfer cross section is predicted to fall off rapidly with increasing energy³; also, the (p,n) reaction at $E > 25$ MeV is well-described by a one-step mechanism. If this expectation is fulfilled, reactions such as $(^{12}\text{C}, ^{12}\text{B})$ and particularly $(^{12}\text{C}, ^{12}\text{N})$ will be very useful spectroscopic tools for the study of Gamow-Teller and other spin-dependent transitions in nuclei.

With the advent of medium-energy heavy-ion (HI) beams, some preliminary work has been started by von Oertzen et al.⁴ with $(^{13}\text{C}, ^{13}\text{N})$ and $(^{13}\text{C}, ^{13}\text{B})$ on ^{12}C at 30 MeV/nucleon. Our study of $(^{12}\text{C}, ^{12}\text{N})$ on the same target nucleus at 35 MeV/nucleon directly addresses the important question of the reaction mechanism.

The experiment was carried out on the S320 spectrograph at NSCL. The angular acceptance of the spectrograph was set at $\pm 0.3^\circ$ which gave a solid angle of 0.25 msr. Particle identification was achieved with a combination of energy-loss, scintillator light output and time of flight signals from the focal plane detector.

Spectra for $^{12}\text{C}(^{12}\text{C}, ^{12}\text{N})^{12}\text{B}$ are shown in Fig. 1. The very broad feature in the 3° spectrum arises from the reaction on the hydrogen contaminant in the target; for angles greater than 3° the $p(^{12}\text{C}, ^{12}\text{N})n$ reaction is not kinematically allowed. The resolution for the ^{12}B states is about 700 keV.

The most prominent feature in the spectra is the peak at 4.5 MeV which corresponds to the

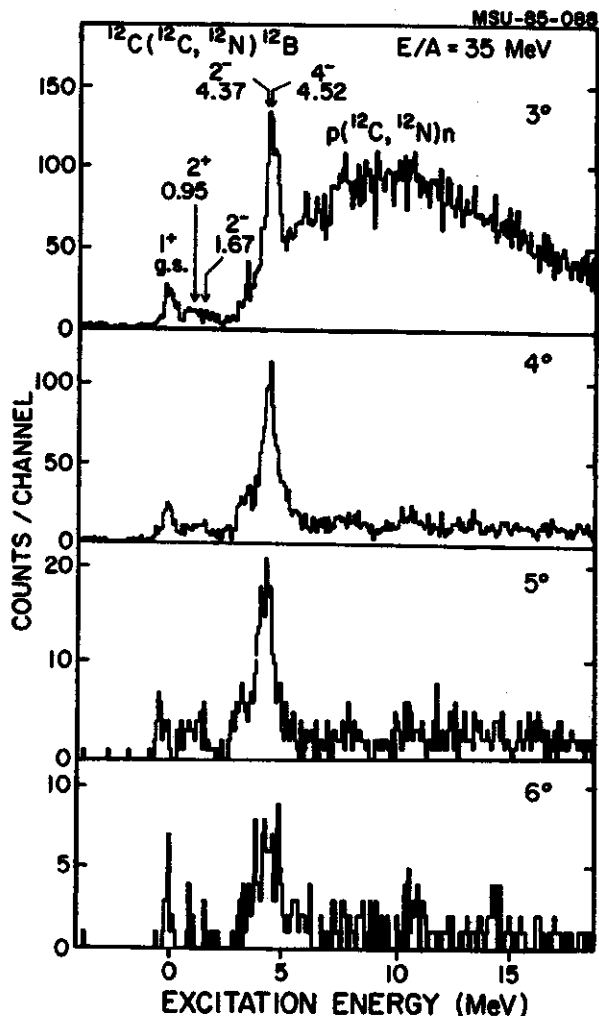


Fig. 1 Spectra for $^{12}\text{C}(^{12}\text{C}, ^{12}\text{N})^{12}\text{B}$ at 35 MeV/nucleon. The spectrograph angle (lab.) is indicated for each case.

unresolved 4^- (4.521 MeV) and 2^- (4.37 MeV) states in ^{12}B . The strength of the peak compared to the low-lying levels and the angular momentum mismatch of the reaction ($\sim 4.5M$) suggests that it is mainly the higher spin state that is contributing; this agrees with our determination of the peak energy. Strong population at this excitation has also been observed in $^{12}\text{C}(d, ^2\text{He})^{12}\text{B}$ by Stahel et al.⁵ and in the mirror nucleus ^{12}N by von Oertzen et al.⁴ Figure 2 is a compressed view of the 4°

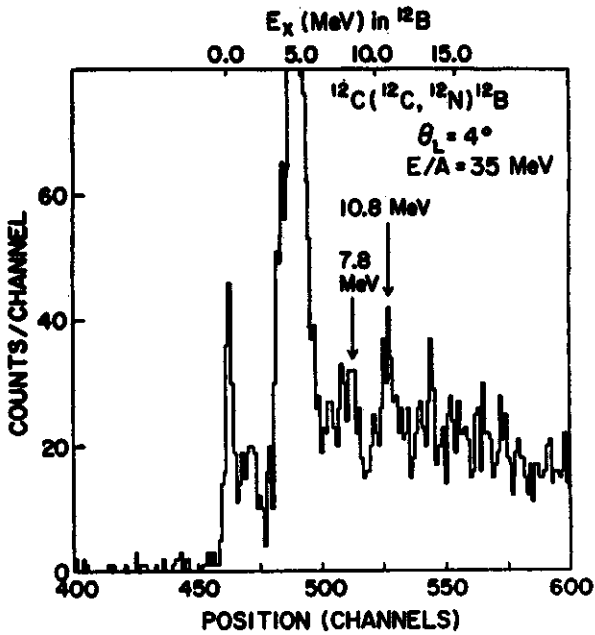


Fig. 2 A compressed view of the 4° spectrum shown in Fig. 1.

spectrum, with neighboring channels added; this shows two broader peaks, one centered at 7.8 MeV and the other at 10.8 MeV. The former is probably the same as observed by von Oertzen et al.⁴ in both ^{12}N and ^{12}B (but seen much more strongly in their case) and lies in the region of the giant dipole resonance.

Microscopic one-step DWBA calculations have been compared with the experimental angular distributions extracted (Fig. 3). The optical potentials for the distorted waves were taken from results of 360 MeV $^{12}\text{C} + ^{12}\text{C}$ elastic scattering⁶. Since the $(^{12}\text{C}, ^{12}\text{N})$ reaction imposes $\Delta S=1$, $\Delta T=1$, only the $V_{\sigma\tau}$ part of the central nucleon-nucleon interaction enters the form-factor (the tensor and exchange terms were not considered here). In the case of the peak at 4.5 MeV, the DWBA predicts a 4^- (4.521 MeV) cross section more than twice that for the 2^- (4.37 MeV) state, in agreement with the kinematic matching argument above.

The required strengths of $V_{\sigma\tau}$ to fit the data are given in Table 1 together with results from other charge-exchange reactions. The most accurate determination of $V_{\sigma\tau}$ in this energy

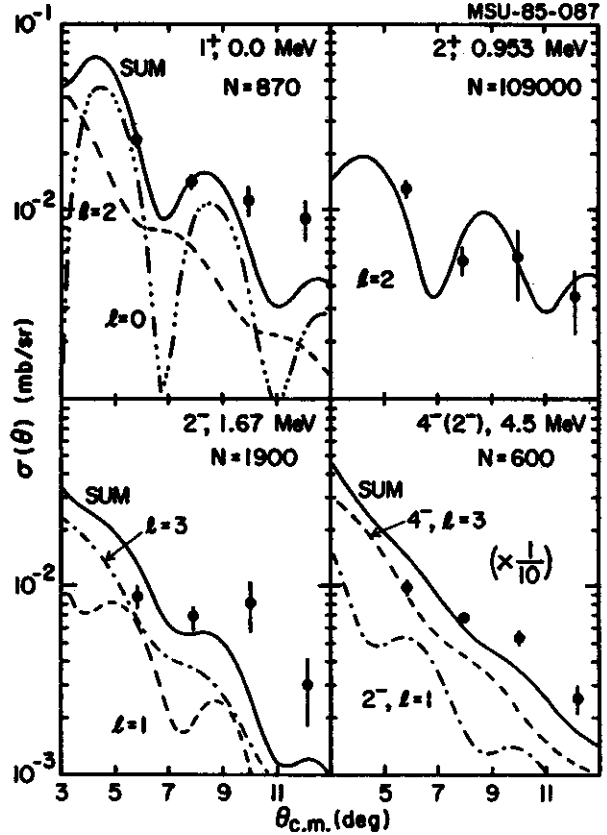


Fig. 3 Angular distributions for the transitions to the states at $E_x = 0.0$ (1^+), 0.953 (2^+), 1.67 (2^-) and 4.5 ($4^-, 2^-$) MeV in ^{12}B . The curves are one-step DWBA calculations with the normalizations N as shown.

Table 1. $V_{\sigma\tau}$ strengths (for a Yukawa interaction with range 1.0 fm)

Reaction	E/A (MeV)	J_f	$V_{\sigma\tau}$ (MeV)	Ref.
$^{12}\text{C}(^{12}\text{C}, ^{12}\text{N})^{12}\text{B}$	35	1^+	30	*
	35	2^+	330	*
	35	2^-	45	*
	35	$4^-(2^-)$	24	*
$(p, n); A = 6-26$	30-50	various	11.7 ± 1.7	7
$^{25,26}\text{Mg}(^6\text{Li}, ^6\text{He})$	6	various	$22-33^{**}$	8
$(^6\text{Li}, ^6\text{He}); A = 18-48$	6	1^+	22-28	9
	6	$3^+, 5^+, 7^+$	20-250	9
$^{28}\text{Si}(^{18}\text{O}, ^{18}\text{F})^{28}\text{Al}$	3	$3^-(2^+)$	76	2
$^{26}\text{Mg}(^{12}\text{C}, ^{12}\text{B})^{26}\text{Al}$	9	$5^+, 3^+$	120, 170	1

*) present work

***) $V_{\sigma\tau} = 17$ (16) MeV when exchange (+ tensor) forces included.

range is probably the average value of 11.7 ± 1.7 MeV obtained from (p,n) studies⁷. While it is true that the present values of $V_{\sigma\tau}$ (with the notable exception of the transition to the 2^+ state) are not as high as other values obtained for $A > 6$ projectiles, there is still a large discrepancy with the accepted $V_{\sigma\tau}$ strength. In terms of cross section, the one-step prediction is almost an order of magnitude smaller than the data (in the case of the 2^+ state it is nearly 3 orders of magnitude smaller). The conclusion is that sequential transfer of nucleons continues to dominate the one-step mechanism at 35 MeV/nucleon. Indeed, if one assumes that the one-step charge exchange cross section is maintained at higher energies but the sequential transfer cross section decreases in the manner suggested by von

Oertzen³, the present results indicate that one would need to go as high as 60 MeV/nucleon before the one-step mechanism predominates.

References

1. A. Etchegoyen et al., Nucl. Phys. A397,343 (1983)
2. B.T. Kim et al., Phys. Rev C 20,1396(1979)
3. W. von Oertzen, GANIL preprint P.84-15
4. W. von Oertzen et al., ISN Grenoble preprint 1984
5. D.P. Stahel et al., Phys. Rev. C 20,1680 (1979)
6. M. Buenerd et al., Nucl. Phys. A424,313 (1984)
7. S.M. Austin, in "The (p,n) Reaction and the Nucleon-Nucleon Force", (ed. Goodman et al.; Plenum, New York, 1980)
8. G. Ciangaru et al., Phys. Lett. 61B,25 (1976)
9. W.R. Wharton and P.T. Debevec, Phys. Rev. C 11,1963(1975)

PARTICLE RESPONSE FUNCTION IN Sm ISOTOPES.

J.E. Duffy, G.M. Crawley, H. van der Plicht, R. Tickle^a, S. Gales^b, E. Gerlic^b, C.P. Massolo^c, J.E. Finck^d.

Most of the work on hole-states¹ has been on medium and heavy nuclei, for both low and high-lying states. Little information is available on the high-lying particle states in medium and heavy nuclei^{2,3}. It would be of interest to see what happens to the single particle strength in this case and compare it to the hole-state¹ case. Theoretical models have been developed to explain the spreading of the single-particle strength by the mixing with both low and high-lying phonon states^{4,5}.

Earlier measurements of particle-states were performed at the IPN, Orsay². We decided to extend the particle-state work to deformed nuclei and use about the same α bombarding energy to study both proton and neutron states. To do this we elected to use the Samarium Isotopes as targets because as the mass increases one goes from a spherical nucleus to a permanently deformed one. The experiment on particle-states in the Samarium Isotopes was performed at the National Superconducting Cyclotron Laboratory (NSCL) using a 100 MeV α beam (charged state 1+). The targets used were ^{144}Sm and $^{148,152,154}\text{Sm}$ with thicknesses of 1 mg/cm^2 and 4 mg/cm^2 respectively. The measurement was carried out using the S320 spectrograph and examined both (α, t) and $(\alpha, ^3\text{He})$ reactions as a means of populating both proton and neutron states in Samarium. It turns out that in the Samarium Isotopes, we will be accessing high spin states like $2f_{5/2}$, $1h_{9/2}$ and $1i_{13/2}$. The S320 detection system allows a 20 MeV excitation energy bite across the focal plane. We need even higher excitation energy for background determination. Two runs of different energy bites are necessary at one angle. This was done for all targets and both reactions at the one angle of 7 degrees (see fig 1).

Distinct differences are observed in the (α, t) spectra as the targets increase in mass and hence deformation (see fig 1). There are also differences in the $(\alpha, ^3\text{He})$ spectra as the targets increase in deformation. In these spectra we see the usual low-lying states and, at higher excitation, above the 3 MeV range one observes additional bound state peaks both in the (α, t) and $(\alpha, ^3\text{He})$ spectra. In the 8-16 MeV

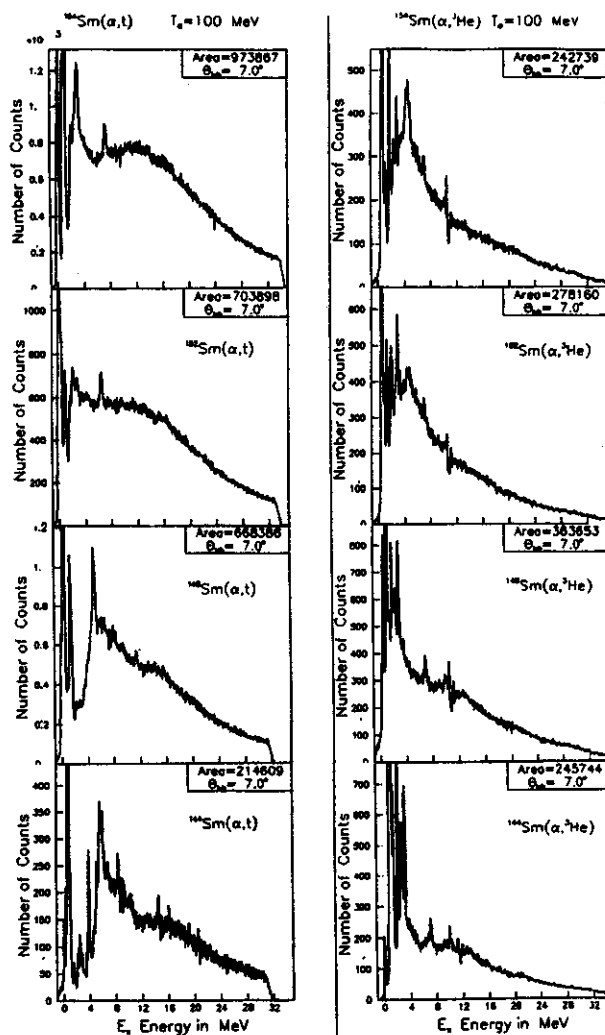


Fig. 1. Spectra of tritons (left) and ^3He (right) scattered from $^{144,148,152,154}\text{Sm}$.

region of excitation energy, in the (α, t) spectra, we observe the development of a broad bump with increasing deformation. We do not observe this phenomenon in the $(\alpha, {}^3\text{He})$ spectra.

Not all of the cross section at high excitation energy comes from single nucleon transfer. Some of the cross section comes from elastic break-up. An elastic α break-up calculation⁶ is shown for the ${}^{148}\text{Sm}(\alpha, t)$ case in Fig. 2. The calculation is normalized to the data at the excitation energy of 30 MeV. This cross section is subtracted from the spectra before further analysis of the data. A similar procedure will be carried out for the other targets and reactions.

The way one analyzed these spectra in the past was to make gaussian fits to different "peaks" in the spectra. This was done for all angles and then one obtained an angular distribution for each of the extracted "peaks". These different "peaks" were compared to DWBA calculations and the single particle strengths were thus obtained. This process of using gaussians is of course somewhat arbitrary. In the present analysis, we plan to take a more objective approach. We take 280 keV slices throughout the whole spectra (instead of making gaussians) and extract an angular distribution for each 280 keV region. By comparing these angular distributions (sliced regions) to DWBA calculations, and the single particle strength as a function of excitation energy can be obtained. The validity of the theoretical models will be shown through the comparison of both the particle strength and the hole strength to those predicted.

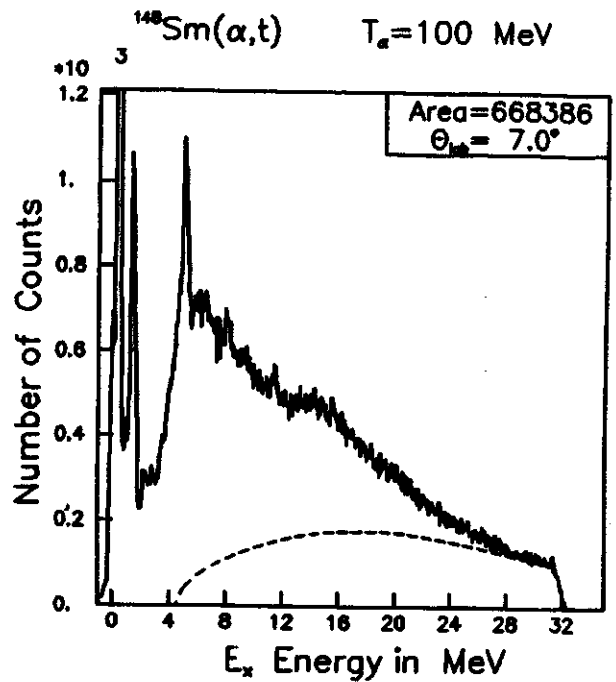


Fig. 2. Spectra of tritons from ${}^{148}\text{Sm}$ with the α -elastic break-up superimposed.

- a University of Michigan
- b Institut de Physique Nucleaire, Orsay, France.
- c INP, Orsay and UNLP/Argentina.
- d Central Michigan University.

1. S. Gales, Nuclear Physics A354, 193c (1981)
2. S. Gales et al, Physical Review C 31, 94 (1985)
3. R.H. Siemssen, J. Phys. Soc. Jpn. 44, 137 (1978)
4. V.G. Soloviev, et al., Nucl. Phys. A342, 261 (1980)
5. G. Bertsch, et al., Phys. Lett. 80B, 167 (1979) and Rev. of Mod. Phys. 55, 287 (1983)
6. J.R. Wu et al, Physical Review C 20, 1284 (1979)

THE TWO-PROTON PICKUP REACTION, (${}^6\text{Li}, {}^8\text{B}$).

A. Saha^a, J.S. Winfield, N. Anantaraman, Z. Chen, R.S. Tickle^b, J. van der Plicht, and H.-L. Wu

Although deeply bound one- and two-neutron hole states have been widely studied¹ and several investigations of deep lying one-proton hole states have been performed², there is almost no information regarding two-proton hole states -- whether deeply bound or not. The basic reason for this is that a two-proton pickup reaction is not possible with light-ions; the lightest case being (${}^6\text{Li}, {}^8\text{B}$). This reaction on the Mo isotopes leading to low-lying levels in the residual nuclei has been studied by Tickle et al.³ at an energy of 15 MeV/nucleon. The aim of the present, exploratory experiment was to determine whether the (${}^6\text{Li}, {}^8\text{B}$) reaction is a useful spectroscopic tool for the study of two-proton hole states, in particular those that

are deeply bound. Some immediate concerns are the widths of the states and the strength with which they are excited relative to the background of continuum states.

A ${}^6\text{Li}$ beam of 35 MeV/nucleon was used to bombard targets of ${}^{12}\text{C}$ and ${}^{148}\text{Sm}$; the main interest being ${}^{148}\text{Sm}({}^6\text{Li}, {}^8\text{B}){}^{146}\text{Nd}$. The S320 spectrograph, set at 5° (lab.), was used to detect the particles of interest. For both targets a group was seen at the expected region for ${}^8\text{B}$ in a plot of energy-loss in the ion chamber (ΔE) against light output from the scintillator (Fig. 1). A gate on this group was used to generate a plot of time-of-flight (TOF) against focal plane position (Figs. 2 and 3). For the case of the ${}^{12}\text{C}$ target, the group

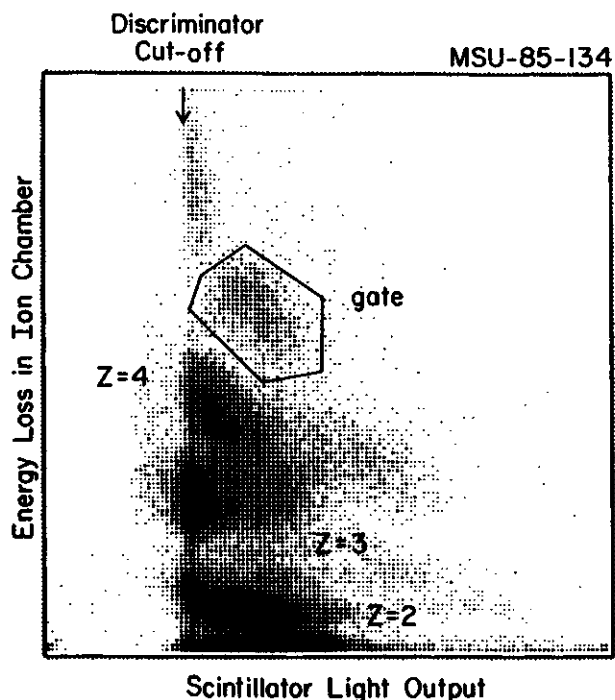


Fig. 1 Plot of energy-loss against scintillator light output for 35 MeV/nucleon ${}^6\text{Li}$ on a ${}^{12}\text{C}$ target. A lower level discriminator on the light output has produced the cut on the left side. The gate is drawn around the particle group which contains ${}^8\text{B}$.

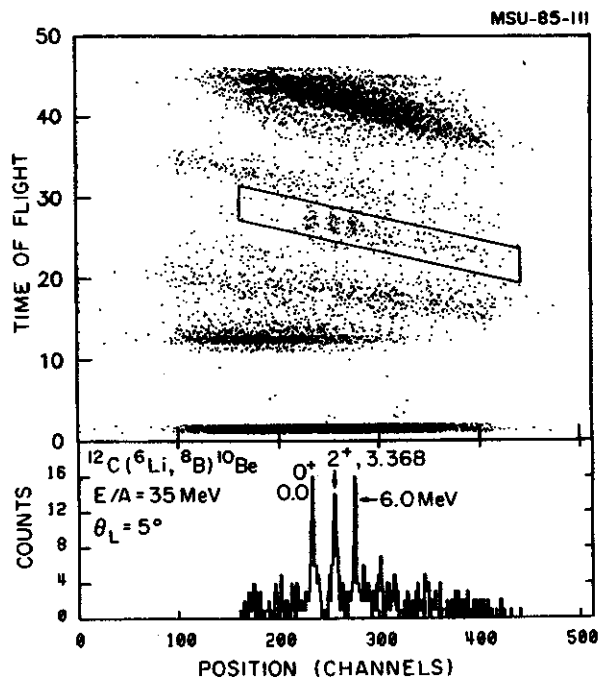


Fig. 2 The upper portion shows a plot of TOF against focal plane position for particles satisfying the gate shown on Fig. 1. The lower portion is a spectrum produced by projecting down the counts inside the box drawn around the ${}^8\text{B}$ group in the 2-d plot. States and excitations in ${}^{10}\text{Be}$ are indicated on this spectrum.

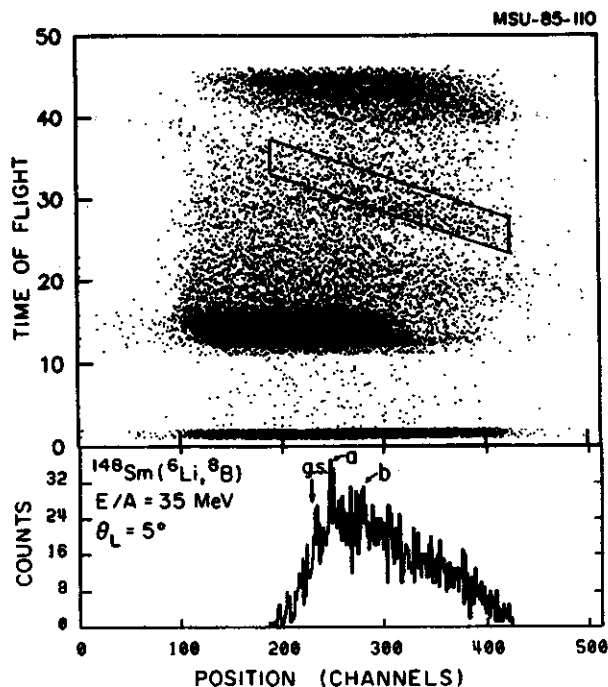


Fig. 3 Similar to Fig. 2 except that the target was ^{148}Sm . The spectrum in the lower portion of the figure was obtained by projecting down the counts within the box. The predicted channel for $^{148}\text{Sm}(^6\text{Li}, ^8\text{B})^{146}\text{Nd}$ is indicated. The peaks labelled (a) and (b) are at approximately 2.5 and 6.8 MeV excitation in ^{146}Nd .

corresponding to ^8B particles could readily be observed. The identity of the other groups, which outnumber the ^8B 's by two orders of magnitude, is uncertain. Both ^7B and ^9B are particle unbound and will not be observed; ^{10}B may account for one of the weaker groups. One possible explanation of the more intense group is that pile-up events caused by the large rate

of breakup of ^6Li , fall in the same region of the ΔE -light plot as the borons.

Three strong peaks appear in the $^{12}\text{C}(^6\text{Li}, ^8\text{B})^{10}\text{Be}$ spectrum; these correspond to the 0^+ ground state, the 2^+ (3.368 MeV) second excited state and a group of levels at 6.0 MeV excitation in ^{10}Be . The cross section for the ground state is $13 \mu\text{b}/\text{sr}$.

While the $^{12}\text{C}(^6\text{Li}, ^8\text{B})^{10}\text{Be}$ spectrum is not particularly clean, the particle identification becomes even less satisfactory with the Sm target (Fig. 3). This may be because the breakup cross section for ^6Li in the Coulomb field of the target is much greater with the higher atomic number. The high background level combined with the low cross section for $^{148}\text{Sm}(^6\text{Li}, ^8\text{B})^{146}\text{Nd}$ -- estimated to be $\sim 0.5 \mu\text{b}/\text{sr}$ for the ground state -- preclude any definite observations. There appears to be some strength excited above background at $E_x \approx 2.5$ and 6.8 MeV, but the main conclusion is that better particle identification and more ^8B counts are required.

a Univ. of Virginia, Charlottesville

b Univ. of Michigan, Ann Arbor

1. For reviews, see G.M. Crawley, Proc. of RCNS Int. Symp., Osaka, Japan, p.590 (1980); S. Gales, Proc. Int. Symp. "HESANS 83", Orsay, France (1983).
2. A. Saha et al., 1977 KVI annual report, p.14; P. Doll et al., Phys. Lett. **82B** 357 (1979).
3. R.S. Tickle et al., Nucl. Phys. **A376** 309 (1982).

THE MASS OF ^{57}Cu

B. Sherrill, K. Beard, W. Benenson, C. Bloch, B.A. Brown, E. Kashy, J.A. Nolen Jr.,
A.D. Panagiotou^a, J. van der Plicht, and J.S. Winfield

In a simple shell model the nucleus ^{57}Cu has one proton outside the ^{56}Ni $N=Z=28$ closed core. Due to the role closed shell nuclei play in nature and hence in nuclear theory, knowledge of the binding energy and structure of ^{57}Cu is important. The mass excess of ^{57}Cu is a direct input into the Garvey-Kelson charge symmetric mass relation ¹. In conjunction with its mirror nucleus ^{57}Ni , ^{57}Cu provides data on the Nolen-Schiffer anomaly ² and hence possible evidence for charge symmetry breaking of the nuclear force. Finally, models of the rp-process, which is hydrogen burning at temperatures near 10^9 K, need the atomic mass excess and level structure of ^{57}Cu to be able to predict the rate of nucleosynthesis of elements with $A > 56$ ³. The rp-process also provides a model for X-ray bursts which depends on the details of ^{57}Cu as well ⁴. Despite the interest in this nucleus, only highly excited states of ^{57}Cu have been observed previously ⁵ in a study of β -delayed proton emission starting from ^{57}Zn and recently, ^{57}Cu β -decay by the reaction $^{58}\text{Ni}(p,2n)^{57}\text{Cu}$ ¹⁴. In this report we describe the first Q value mass measurement of ^{57}Cu and the first use of the $(^7\text{Li},^6\text{He})$ exotic transfer reaction.

The measurements were performed at the National Superconducting Cyclotron Laboratory (NSCL) with the S320 spectrograph, which has a quadrupole-quadrupole-dipole-sextupole configuration and a solid angle of 0.5 msr. The mass of ^{57}Cu was measured by determining the Q value of the reaction $^{56}\text{Ni}(^7\text{Li},^6\text{He})^{57}\text{Cu}$ relative to known Q values. The 173.6 MeV ^7Li beam was provided by the K500 cyclotron. The target was a 3.77 mg/cm² foil of 99.93% enriched ^{56}Ni . The standard S320 focal plane detector was used. The event trigger was an anode signal from the plastic scintillator above a discriminator level. The S320 focal plane was calibrated with $^{56}\text{Ni}(^7\text{Li}^{3+}, ^7\text{Li}^{2+})$ elastic scattering. The ratio

of $^7\text{Li}^{3+}$ to $^7\text{Li}^{2+}$ was found to be approximately 9×10^{-5} . The calibration was checked by comparing the known ⁶ excited states in ^{56}Cu with ones measured via the $^{56}\text{Ni}(^7\text{Li},^6\text{He})^{56}\text{Cu}$ reaction. The rms deviation of this comparison was 20 keV, mostly due to uncertainties in resolving states in ^{56}Cu and magnet scaling. The ^7Li beam energy was measured by the difference in focal plane position between the $^7\text{Li}^{2+}$ elastic peak and the ^6He peak from the reaction $^{27}\text{Al}(^7\text{Li},^6\text{He})^{26}\text{Si}(\text{g.s.})$, and was accurate to 200 keV. Further, since the $^{27}\text{Al}(^7\text{Li},^6\text{He})^{26}\text{Si}$ Q value is well known ⁷, and the magnetic fields were the same as used for the $^{56}\text{Ni}(^7\text{Li},^6\text{He})^{57}\text{Cu}$ reaction, this also provided a Q value calibration for the ^{57}Cu mass measurement.

The spectra obtained from the $^{56}\text{Ni}(^7\text{Li},^6\text{He})^{57}\text{Cu}$ and $^{27}\text{Al}(^7\text{Li},^6\text{He})^{26}\text{Si}$ reactions are shown in fig. 1. The absence of

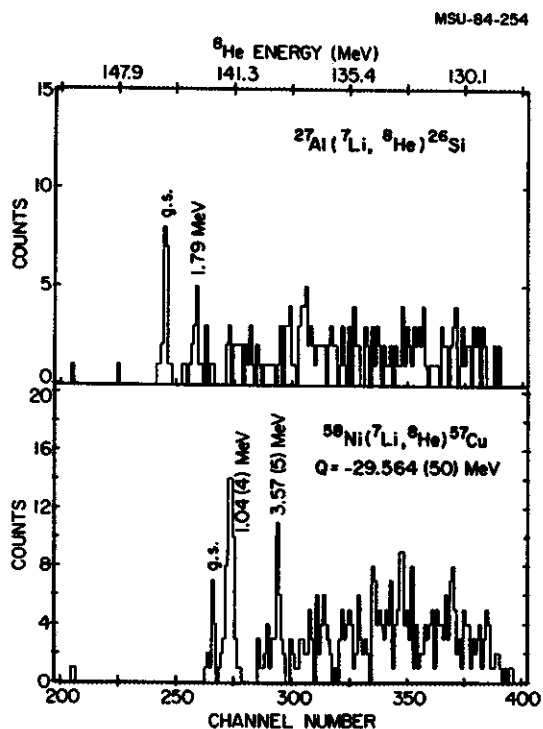


Fig. 1: Position spectra for the measured ^6He nuclei.

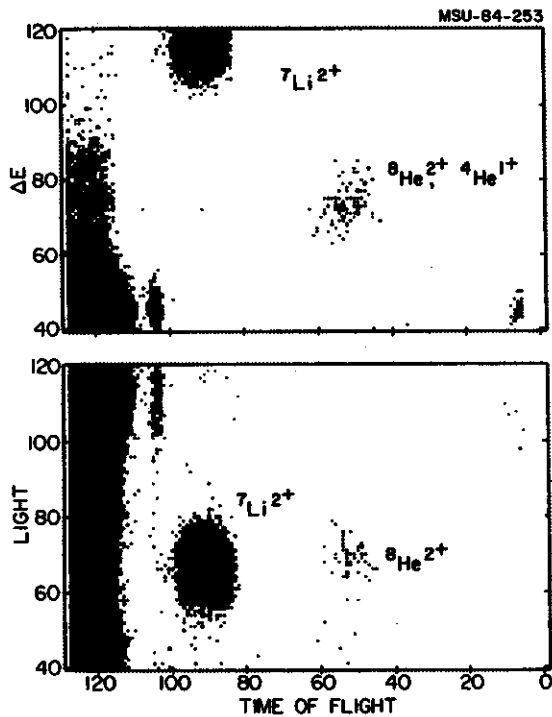


Fig. 2: Particle identification for the ${}^8\text{He}$ reaction products. The units are arbitrary with the time axis corresponding to 1 nsec/channel.

counts below the lowest observed state in ${}^{57}\text{Cu}$ indicates good ${}^8\text{He}$ particle identification, which is shown in fig. 2. Assuming the state at lowest excitation energy is the ${}^{57}\text{Cu}$ ground state, we measured a Q value of $-29.564(50)$ MeV, which leads to a mass excess for ${}^{57}\text{Cu}$ of $-47.35(5)$ MeV. This value agrees with the Janecke-Garvey-Kelson ${}^{\circ}$ mass excess prediction of -47.43 MeV. This value also agrees with a β -endpoint measurement by Shinozuka et al.¹⁴ of $\text{ME}({}^{57}\text{Cu}) = -47.34(13)$ MeV. The error in the measurement comes primarily from the statistical uncertainties in the centroid of the ${}^{26}\text{Si}$ g.s. and ${}^{57}\text{Cu}$ g.s. peaks. These uncertainties added in quadrature give 36 keV. The other two major sources of error are: 24 keV from uncertainty in the beam energy, and 20 keV from the uncertainty in the focal plane calibration.

Fig. 3 shows the measured levels of ${}^{57}\text{Cu}$ relative to its mirror nucleus, ${}^{57}\text{Ni}$. The $1/2^-$ and the $5/2^-$ states are expected to lie within 50 keV of each other according to calculations of the displacement energies of these states and

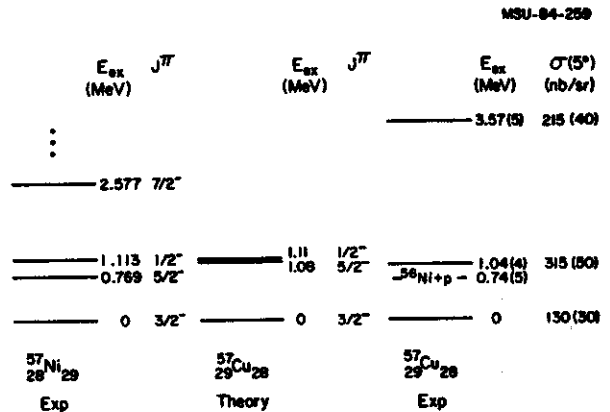


Fig. 3: Level diagrams for ${}^{57}\text{Ni}$ and ${}^{57}\text{Cu}$. The theory used to predict the structure of ${}^{57}\text{Cu}$ is described in the text. The measured state in ${}^{57}\text{Cu}$ at 1.04(4) MeV is probably the $5/2^-$ and $1/2^-$ states unresolved.

the structure of the mirror nucleus. The calculations of the displacement energies reproduce quite well the trends in nearby nuclei and will be discussed below in connection with the Nolen-Schiffer anomaly. A statistical analysis of the peak at 1.04 MeV shows that its width is identical to that expected from the spectrograph resolution and the finite target thickness. However, a strong selectivity of the (${}^7\text{Li}, {}^8\text{He}$) reaction for one of these states and not the other is not expected because the states are both single particle in composition. Also, since the angular momentum mismatch between the incoming and outgoing particles is only 1.4 h there should not be the preference for high spin states which is usually the case for heavy-ion induced reactions⁹. Therefore for the purposes of this analysis, we will assume the $1/2^-$ and the $5/2^-$ states both lie at 1.04(4) MeV excitation. The quoted uncertainty in the excitation energy of these states is larger than the statistical error because of uncertainty in separating the states. It is possible that only one of the states is populated, in which case the excitation of the other would be unknown.

The mirror pair ${}^{57}\text{Ni}$ - ${}^{57}\text{Cu}$ permit a test for the Nolen-Schiffer anomaly. The Nolen-Schiffer anomaly is the systematic discrepancy between the Coulomb displacement energy calculated from

theory, assuming charge symmetry of the nuclear force, and the displacement energy measured experimentally. For mirror systems the Coulomb displacement energy is defined as:

$$E_C = Z_> - Z_< + \Delta_{nh}$$

where $Z_>$ and $Z_<$ are the atomic mass excesses of the proton rich and the neutron rich members of the pair, respectively; and Δ_{nh} is the neutron-hydrogen mass difference. The anomaly is particularly surprising because the Coulomb force is well known, and its effect on nuclear binding energies should be calculable. Two possible explanations for this anomaly are nuclear structure effects not included in the calculations and charge symmetry breaking in the nucleon-nucleon force. A case such as the A=57 pair provides valuable data because the closed ^{56}Ni core allows detailed nuclear structure calculations to be made, as has been done for other single particle or single hole nuclei.

It is interesting to compare the present displacement energy and those of other mirror states from A=41 to 59 to a standard theoretical model which takes into account the Coulomb interaction between the valence and core nucleons along with some well understood corrections^{10,11}. The ratios of the experimental displacement energies over those calculated with this model are shown in Fig. 4. We include in this comparison the displacement energies of other states in the A>39 mass region which can be considered as single-particle or single-hole states. The persistence of the anomaly over this range of A and orbit can be taken as evidence for charge symmetry breaking in the nuclear force.

Finally, the structure of ^{57}Cu is interesting because of its importance in the rp-process in element production with A > 56. The rp-process is proton burning via the (p, γ) reaction at temperatures between $T_9 = 0.10$ and 2.0, where T_9 is the temperature in units of 10^9 K. A detailed study of the rp-process by Wallace and Woosley³ found that the nucleus ^{57}Cu is an important branch point from lower- to higher-A nuclei because of the stability and

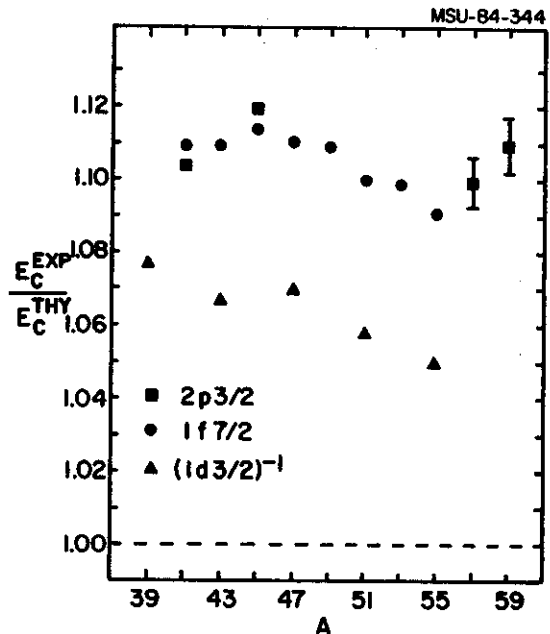


Fig. 4: The ratio of experimental displacement energies to those calculated with the model described in the text plotted vs. A.

long stellar half life of ^{56}Ni . The rate of higher-A production may also be a critical factor in energy production from X-ray bursts which result from hydrogen accreted onto the surface of white dwarfs or neutron stars^{12, 13}. The crucial reaction, $^{56}\text{Ni}(p,\gamma)^{57}\text{Cu}$, will be dominated by (p, γ) resonances, and therefore the reaction rate is sensitive to the proton energy of these resonances. The present experiment shows that the nucleus ^{57}Cu is proton bound by 0.74(5) MeV, hence there is an l=1 resonance at 0.30(4) MeV. There is also an l=3 resonance at about the same energy, but the larger angular momentum barrier will significantly reduce its importance. Wallace and Woosley also included a resonance at 1.752 MeV on which our study has no information. However photodisintegration of ^{57}Cu dominates its production at the higher temperatures at which this resonance would be important. At temperatures up to $T_9 = 1.0$ only the lower energy resonance is important. The l=1 resonance energy is only 0.12 MeV different from the that originally assumed by Wallace and Woosley but leads to a significant deviation from the previously calculated $^{56}\text{Ni}(p,\gamma)^{57}\text{Cu}$

rate. A further correction to the ^{57}Cu production rate will be due to the influence of the inverse reaction, $^{57}\text{Cu}(\gamma, p)^{56}\text{Ni}$. With the new mass excess for ^{57}Cu we calculate the Q value for the $^{57}\text{Cu}(\gamma, p)^{56}\text{Ni}$ reaction to be $-0.74(5)$ MeV instead of the -0.69 MeV assumed by Wallace and Woosley. This implies a decrease in the (γ, p) photodisintegration rate. The ratio of the recalculated $^{56}\text{Ni}(p, \gamma)^{57}\text{Cu}$ rate to the previously calculated rate $\lambda_{p\gamma}$ vs. temperature is shown in fig. 5. The dashed curves were calculated for the resonance energy changed by ± 40 keV. The deviation from unity shown in fig. 5 is due to the narrower proton decay width of

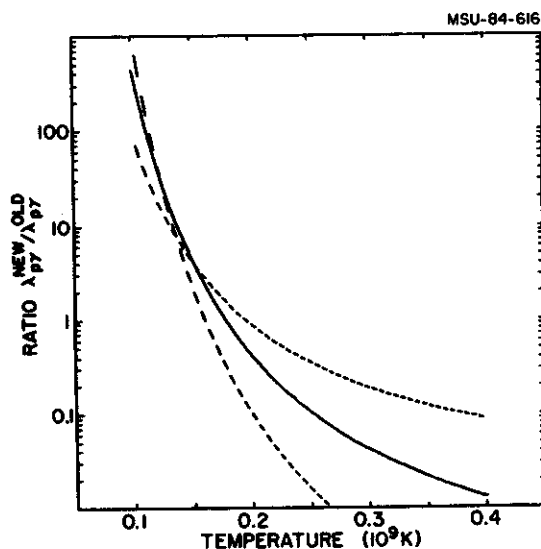


Fig. 5: The ratio of the recalculated $^{56}\text{Ni}(p, \gamma)^{57}\text{Cu}$ rate in units of $\text{cm}^3/\text{mole-sec}$ to the previously calculated rate vs. temperature. The dashed lines were calculated by varying the resonance energy by the uncertainty in the measurement, ± 40 keV.

the resonance and the decreased resonance energy.

In conclusion, the ^{57}Cu mass excess and level structure deduced from this experiment yield two diverse and significant results.

First, there is additional evidence on the Nolen-Schiffer anomaly which may indicate charge symmetry breaking of the nuclear force in mirror systems. When detailed nuclear structure calculations are performed, they fail to reproduce the measured Coulomb energy shift by about 10% for single particle states, and at least 5% for hole states. If indeed all significant structure effects have been included, then the most probable cause of the anomaly must be charge asymmetric forces. Second, the measured Coulomb shifts of the levels in ^{57}Cu indicate that recalculations of the rp-process will change the production rates of elements with $A > 56$.

a On leave from Department of Physics, University of Athens, Athens, Greece

References

1. I. Kelson and G.T. Garvey, Phys. Lett. 23, 689(1966).
2. J.A. Nolen, Jr. and J.P. Schiffer, Annu. Rev. Nucl. Sci. 19, 471(1969).
3. R.K. Wallace and S.E. Woosley, Ap. J. Supp. 45, 389(1981).
4. R.K. Wallace and S.E. Woosley, AIP Conf. Proc. No. 115 (AIP, New York, 1984) p.319.
5. D.J. Vieira et al., Phys. Lett. 60B, 261(1976).
6. C.M. Lederer and V.S. Shirley Ed., Table of Isotopes (Wiley, New York, 1978).
7. A.H. Wapstra and G. Audi, 1983 Atomic Mass Table, to be published in Nucl. Phys. A.
8. S. Maripuu, special ed., At. Data Nucl. Data Tables 17, 493(1976).
9. D.M. Brink, Phys. Lett. 40B, 36(1972).
10. B. Sherrill et al., Phys. Rev. C28, 1712(1983).
11. B. Sherrill et al., Phys. Rev. C31, 875(1985).
12. R.K. Wallace, S.E. Woosley, and T.A. Weaver, Ap. J. 258, 696(1982).
13. M. Hashimoto, T. Hanawa and D. Sugimoto, Publ. Astron. Soc. Japan 35, 1 (1983).
14. T. Shinozuka et al., Phys. Rev. C30, 2111(1984).

RECENT MASS MEASUREMENTS OF PROTON RICH NUCLEI: ^{39}Sc and ^{39}Ga

B. Sherrill, C. Bloch, W. Benenson, E. Kashy, M. Lowe, J.A. Nolen Jr.,
J. van der Plicht, J. Stevenson, J.S. Winfield.

The success of the ^{67}Cu mass measurement¹ from the Q value of the $^{66}\text{Ni}(^7\text{Li},^4\text{He})^{67}\text{Cu}$ reaction has encouraged a continuation of the program of mass measurements using heavy-ion transfer reactions with beams from the K500 cyclotron. Two cases which have been studied recently are the reactions $^{40}\text{Ca}(^7\text{Li},^4\text{He})^{39}\text{Sc}$ and $^{66}\text{Ni}(^{12}\text{C},^9\text{Li})^{61}\text{Ga}$. Nothing was known previously about either ^{61}Ga or ^{39}Sc , the latter nucleus was thought to be a candidate for ground-state proton decay. Knowledge of its mass excess would indicate whether this is true and whether the lifetime is long enough to be measured. The ground state mass excess of ^{39}Sc would also make the third known member of the A-39 isobaric quartet, which would allow the systematics of IMME b and c coefficients² to be extended to A-39. In general, knowledge of the nature of nuclei around the doubly magic nucleus ^{40}Ca provides shell model data for interactions within, and mixing between, the sd and fp shells. The nucleus ^{61}Ga is a mirror nucleus and hence its mass and level structure are important in a variety of studies including isospin mixing, the Nolen-Schiffer anomaly³, β decay, and in some astrophysical calculations involving proton rich nuclei⁴.

The analysis is still in progress for ^{61}Ga , but preliminary indications are not promising that we will be able to determine a mass. The cross section for the $^{66}\text{Ni}(^{12}\text{C},^9\text{Li})$ reaction, which was measured at 3 degrees and with a $^{12}\text{C}^{3+}$ beam energy of 15 MeV/A, appears to be below 50 nb/sr. With the S320 spectrograph it is possible to measure the Q value of reactions with cross sections as low as this or lower. However in this case an analog beam, $^{16}\text{O}^{4+}$, was present in amounts which may have been as high as 10% of the total beam current and created a constant background in the ^9Li spectra. This

background process had approximately the same cross section as the reaction of interest and made identification of the ^{61}Ga ground state difficult. Although we are presently unable to determine a ^{61}Ga mass, we can conclude that it appears the measurement of the ^{61}Ga mass is possible using a 3 proton transfer reaction provided there are no significant contaminants in the spectra. Possible reactions which would be free of analog beams are for example $(^{14}\text{N},^{11}\text{Be})$ or $(^{11}\text{B},^4\text{He})$.

In contrast to the problems encountered in the ^{61}Ga measurement, the ^{39}Sc measurement went well. These measurements were performed with a 24.7 MeV/u ^7Li beam produced by the K500 cyclotron. The ^4He reaction products from the $^{40}\text{Ca}(^7\text{Li},^4\text{He})$ reaction were analysed with the S320 spectrograph set at 4 degrees. The target was a 5.8(2) mg/cm² 99.96% enriched ^{40}Ca foil, which was made at the NSCL by reduction of CaCO_3 and evaporation of the metal onto a glass slide. The target thickness was measured by observing the difference in energy loss for elastic scattering from a ^9Be target of known thickness compared to that from the ^{40}Ca target. This technique was checked by an alpha gauge measurement of the ^{40}Ca target thickness. The focal plane was calibrated with $^7\text{Li}^{2+}$ elastic scattering (which fell in the detector at the same field setting as the ^4He ions of interest) and by the known Q value of the $^9\text{Be}(^7\text{Li},^4\text{He})^8\text{B}$ reaction. Further, the ^7Li beam energy was measured by the observed difference in focal plane position of the $^7\text{Li}^{2+}$ elastic and the ^8B ground state peak. The beam energy was found to be $E/A = 24.66(1)$ MeV.

The spectra for the $^{40}\text{Ca}(^7\text{Li},^4\text{He})^{39}\text{Sc}$ and $^9\text{Be}(^7\text{Li},^4\text{He})^8\text{B}$ reactions are shown in Figure 1. The observed states in ^8B at 0.78 and 2.32 MeV correspond to previously known states³. The few

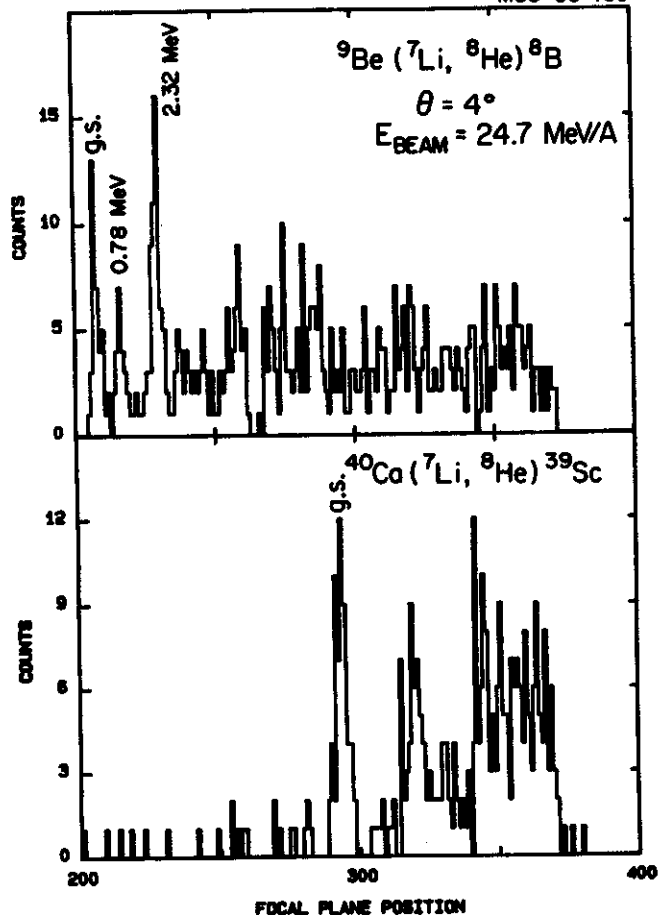


Fig. 1 Position Spectra for the ${}^9\text{He}$ reaction products.

background counts above the ${}^{39}\text{Sc}$ ground state may arise from the reactions on Zr, which was used as a reducing agent in the Ca evaporation process, present in the target. The measured Q value for the reaction is $-37.24(5)$ MeV. The corresponding ${}^{39}\text{Sc}$ mass excess is $-14.30(5)$ MeV. The quoted error includes uncertainties in target thickness, calibration, and centroid determination. We estimate the cross section

for this reaction at 4 degrees to be $.11(1)$ $\mu\text{b}/\text{sr}$.

The mass excess implies that ${}^{39}\text{Sc}$ is proton unbound by $470(50)$ keV. Despite the relatively high spin, $7/2^-$, of the ground state (the spin is assumed to be the same as the ground state spin of ${}^{39}\text{Ar}$, the analog of ${}^{39}\text{Sc}$), the proton decay energy of 470 keV implies a lifetime on the order of 10^{-14} sec. This lifetime is too short to be observed by standard decay techniques. The decay width should be a few eV, which would in itself be difficult to measure. We thus conclude ${}^{39}\text{Sc}$ is not a candidate for long lived proton decay.

Using the measured mass excess of ${}^{39}\text{Sc}$ and other known $T=3/2$; $7/2^-$ states in $A=39$ nuclei we can extract the b and c coefficients from the IMME equation². We find

$$b = 6.31(1) \text{ MeV, and}$$

$$c = 166(9) \text{ keV.}$$

These values agree with the systematics established for $A=9$ to $A=37$.

The relatively large yield for the (${}^7\text{Li}, {}^8\text{He}$) reaction indicates it may be a useful tool for studying masses and excitation spectra of other exotic proton rich nuclei.

References

1. B. Sherrill et al., Phys. Rev. **C31**, 875(1985).
2. W. Benenson and E. Kashy, Rev. Mod. Phys. **51**, 527(1979).
3. J.A. Nolen Jr. and J.P. Schiffer, Annu. Rev. Nucl. Sci. **19**, 471(1969).
4. R.K. Wallace and S.E. Woosley, AIP Conf. Proc. No. 115 (AIP, New York, 1984) p.319.
5. F. Ajzenberg-Selove, Nucl. Phys. **A413**, 101(1984).
6. P.M. Endt and C. vanderLeun, Nucl. Phys. **A310**, 1(1978).

MASSES OF ^{47}Ar AND ^{51}Ca USING A ^{14}C BEAM AND A ^{48}Ca TARGET

B. Sherrill, C. Bloch, W. Benenson, K. Beard, E. Kashy, J. vanderPlicht, J.S. Winfield,
A.D. Panagiotou^a, C. Thorn^b.

Recently there has been interest in studying the region of neutron rich nuclei beyond ^{48}Ca . This interest was generated by the prediction of Tondeur¹ that ^{52}Ca is doubly magic. A review of the literature indicates that little is known about Ca isotopes heavier than ^{48}Ca and other lighter elements with $N > 28$. To extend the knowledge of this region, we proposed to use the ^{14}C beam available from the Brookhaven National Laboratory Tandem to bombard a ^{48}Ca target and study a series of reactions leading to very neutron rich nuclei. However, due to contaminants in the ^{48}Ca target, primarily ^{40}Ca , we were only marginally successful in two attempts: the $^{48}\text{Ca}(^{14}\text{C},^{15}\text{O})^{47}\text{Ar}$ and $^{48}\text{Ca}(^{14}\text{C},^{11}\text{C})^{51}\text{Ca}$ reactions.

The reactions were studied in the QDDD spectrometer at the BNL tandem and with ^{14}C energies ranging from 100 to 110 MeV. The target thicknesses were measured with the spectrograph set at 0 degrees and the $^{14}\text{C}^{6+}$ beam attenuated to approximately 1000 particles/sec. The target thicknesses were calculated based on the shift of the elastic peak with the target in and target out. The focal plane was calibrated with $^{14}\text{C}^{6+}$ elastic scattering at somewhat lower magnetic fields than those used to perform the mass measurements. Corrections for field scaling were taken from previous work². These corrections and the calibration were checked by measuring the Q values of known reactions, for example $^{48}\text{Ca}(^{14}\text{C},^{12}\text{C})^{50}\text{Ca}$ and $^{48}\text{Ca}(^{14}\text{C},^{15}\text{N})^{47}\text{K}$. The uncertainties in the measured Q values due to the calibration was estimated to be less than 20 keV. Particle identification was done by gating groups from a ΔE -E map generated by the QDDD detector and was generally very clean.

The purpose of the first study was to produce and measure the mass of ^{47}Ar .

Previously, ^{47}Ar had not been observed even in stability studies. The spectrum for the $^{48}\text{Ca}(^{14}\text{C},^{15}\text{O})^{47}\text{Ar}$ reaction at $\theta=10$ deg is shown in figure 1. In this case the spectrum is dominated by ^{15}O ions from ^{12}C and ^{16}O contaminants in the target. There is an indication for the ^{47}Ar ground state(g.s.) peak which corresponds to a Q value of $-18.14(10)$ MeV with a cross section of $0.6(2)$ $\mu\text{b}/\text{sr}$. This Q value yields a mass excess for ^{47}Ar of $-25.91(10)$ MeV. The uncertainty is dominated by background subtraction.

In an attempt to verify this measurement, the experiment was repeated at $\theta=21$ degrees. The spectrum from this run is shown in figure 2. As shown in the figure the ^{16}O and ^{12}C contaminants have moved to higher ^{47}Ar excitation due to reaction kinematics. The poor

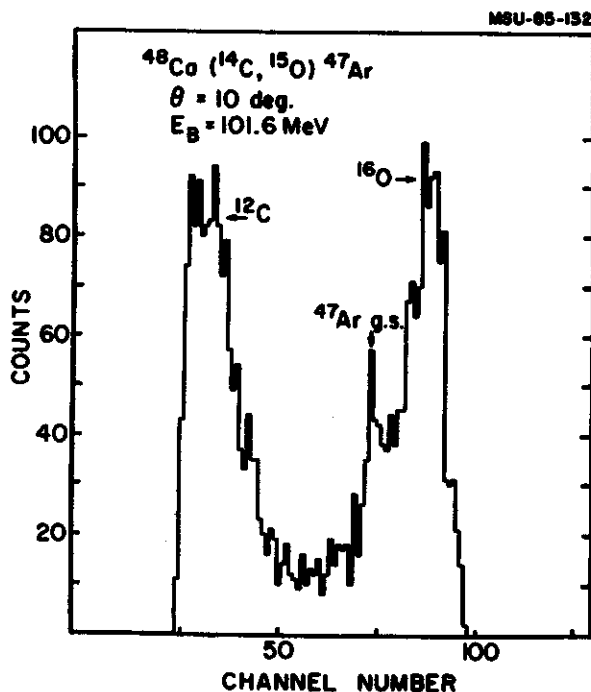


Fig. 1 Position spectrum from the $^{48}\text{Ca}(^{14}\text{C},^{15}\text{O})^{47}\text{Ar}$ reaction taken at 10 degrees.

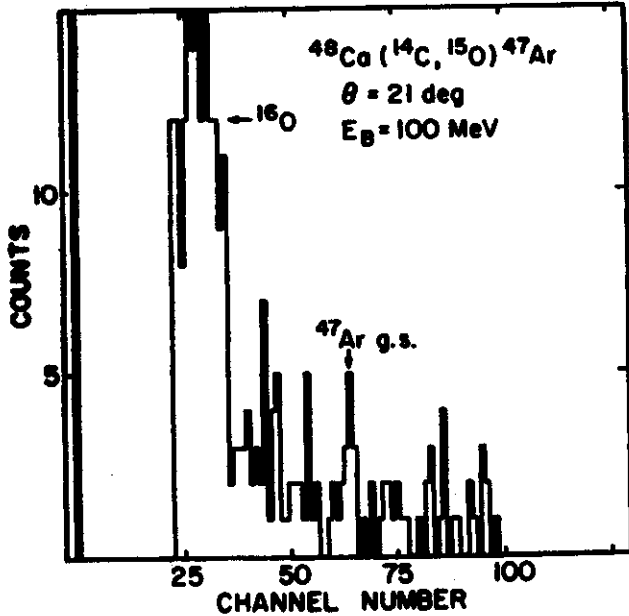


Fig. 2 Position spectrum from the $^{48}\text{Ca}(^{14}\text{C}, ^{15}\text{O})^{47}\text{Ar}$ reaction taken at 21 degrees.

statistics and background from contaminants in the ^{48}Ca target make definite conclusions on the existence of a ^{47}Ar g.s. peak difficult. The candidate marked in the figure corresponds to a Q value of $-18.0(2)$ MeV and a cross section of $0.08(6)$ $\mu\text{b}/\text{sr}$. This would lead to a ^{47}Ar mass excess of $-25.8(2)$ MeV, in agreement with the 10 degree data. Based on this data, we tentatively take the mass excess of ^{47}Ar as the weighted average of the two measurements, $-25.9(1)$ MeV. This mass excess is compared to predictions taken from the compilation of

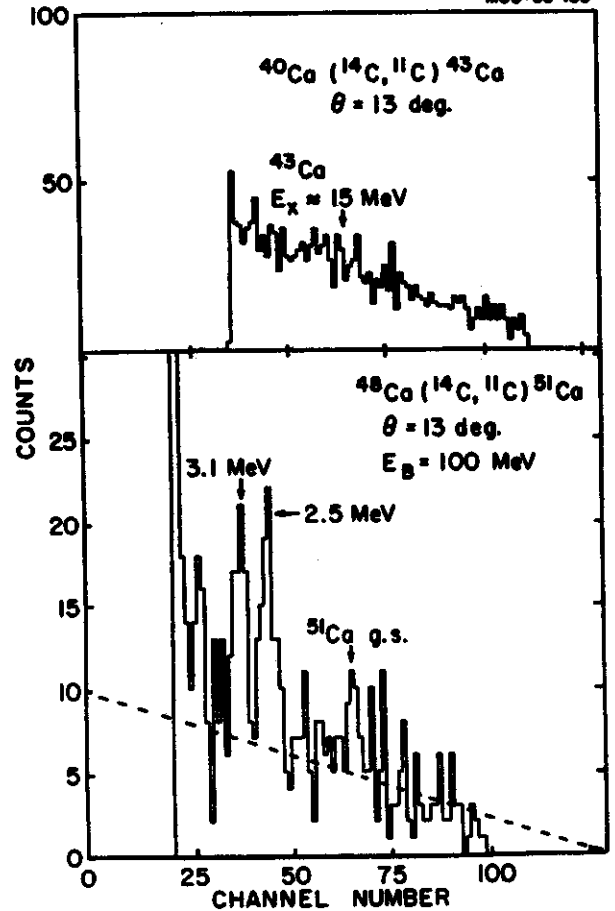


Fig. 3 Position spectrum from the $^{48}\text{Ca}(^{14}\text{C}, ^{11}\text{C})^{51}\text{Ca}$ reaction and the measurement of ^{11}C ions from ^{40}Ca impurities in the ^{48}Ca target. The dashed line is a fit to the ^{40}Ca target data.

Maripuu³ in table 1. There is good agreement with the models predictions.

Table 1: Comparison of the measured ^{47}Ar mass to various mass predictions.

Model	Mass Excess (MeV)
Myers	-25.08
Groote-Hilf-Takahashi	-26.18
Beiner-Lombard-Mass	-25.0
Janecke-Garvey-Kelson	-25.82
Comay-Kelson	-25.70
Experiment	-25.91(10)

The second nucleus studied was ^{51}Ca . The spectrum for the $^{40}\text{Ca}(^{14}\text{C}, ^{11}\text{C})^{51}\text{Ca}$ spectrum, taken at $\theta=13$ degrees, is shown in figure 3. Also shown in the figure is data taken from the $^{40}\text{Ca}(^{14}\text{C}, ^{11}\text{C})^{43}\text{Ca}$ reaction at the same spectrograph settings, which corresponds to approximately 15 MeV excitation in ^{43}Ca at the center of the focal plane. The vertical scale was adjusted to represent the ^{11}C yield expected from the 4% ^{40}Ca in the ^{43}Ca target plotted on the same scale as the data taken in runs using the ^{40}Ca target. Based on this data we conclude that most of the counts seen in the lower spectrum are due to the ^{40}Ca impurity. The dashed line is a fit to the $^{40}\text{Ca}(^{14}\text{C}, ^{11}\text{C})^{43}\text{Ca}$ data scaled for the integrated beam current, target thicknesses, and isotopic abundances. Assuming the lowest state observed is the g.s. of ^{51}Ca we obtain a Q value of $-16.93(10)$ MeV, which corresponds to a ^{51}Ca mass excess of $-34.96(10)$ MeV. We also see two more strongly populated states which lie at 2.5 and 3.1 MeV.

Brauner et al.⁴ have recently published a mass measurement of ^{51}Ca from the $^{40}\text{Ca}(^{18}\text{O}, ^{15}\text{O})^{51}\text{Ca}$ reaction at a beam energy of 102 MeV. In their experiment they also used a 96% enriched ^{40}Ca target, with the major isotopic contaminant of ^{42}Ca . However, they claim to see no background from the ^{40}Ca impurity which for their system and beam energy would yield ^{11}C ions at around 12 MeV excitation in ^{43}Ca . Thus, they interpret all ^{11}C ions as corresponding to ^{51}Ca . With this assumption they measure an excitation spectrum shown in figure 4. Also shown in the figure is the excitation spectrum obtained in our experiment and that calculated with a shell model assuming a closed ^{40}Ca core and an active $1f_{7/2}$ proton orbit and active $2p_{3/2}, 2p_{1/2}$, and $1f_{5/2}$ neutron orbits. The matrix elements for this model space were taken from references 5 and 6. This shell model reproduces the low lying excitation spectra for known nearby nuclei. The predicted mass excess from the shell model of $-35.2(2)$ MeV also agrees with the Garvey-Kelson prediction of -35.15 MeV. These two predictions agree with

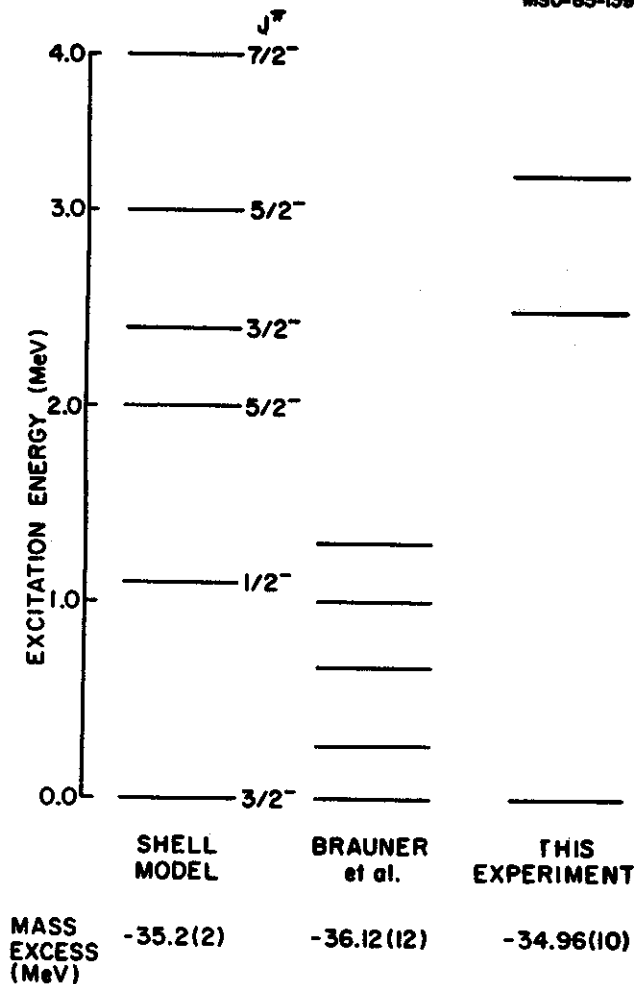


Fig. 4 Comparison of the ^{51}Ca excitation spectrum measured by Brauner et al., this experiment, and calculated assuming the shell model described in the text.

our measurement of the mass excess, but disagree by almost one MeV from the Brauner value. Along with the mass excess, the observation of several states with excitation energy below 1 MeV by Brauner is difficult to understand in light of the shell model prediction. If their interpretation is correct it indicates a significant deviation in the shell structure of ^{51}Ca from nearby nuclei. Our data do not indicate this deviation, but it is possible that the states seen by Brauner are lost in the background in our ^{51}Ca spectrum. Clearly, the discrepancies surrounding this nucleus warrant its further study.

1. F. Tondeur, Proc. 4th Intern. Conf. on Nuclei Far From Stability (Helsingør, 1981) CERN-Report 81-09, p. 81.
2. C. Thorn et al., Phys. Rev. C25, 331(1982).
3. S. Maripuu, special ed., At. Data Nucl. Data Tables 17, 494(1976).
4. M. Brauner, D. Rychel, R. Gyufko, C.A. Wiedner, and S.T. Thornton, Phys. Letts. 150B, 75(1985).
5. H. Horie and K. Ogawa, Prog. of Theor. Physics 46, 439(1971).
6. H. Horie and K. Ogawa, Nucl. Phys. A216, 407(1973).

IN-BEAM γ -RAY SPECTROSCOPY OF NEUTRON-DEFICIENT ODD-ODD Re NUCLEI

J. E. Kupstas-Guido, W. Olivier, W.-T. Chou and Wm. C. McHarris.

Very little in-beam gamma-ray spectroscopy has been done on odd-odd systems, primarily because it was thought that such systems were complicated to the point of diminishing returns. This seems to be the case for spherical odd-odd nuclei, but recent results [1] on the deformed odd-odd nucleus, ^{182}Re , indicate otherwise. In Figure 1 is shown the relatively simple level scheme that resulted from the $^{181}\text{Ta}(\alpha, 3n\gamma)^{182}\text{Re}$ reaction. Some 90% of the deexcitation funnels down through only two rotational bands, with most of the rest proceeding through two additional bands.

Deformed odd-odd nuclei are prime candidates for in-beam gamma-ray studies for several reasons: 1) Their spectra are much

simpler than previously thought. 2) Coriolis couplings and distortions are at a maximum, including the self-coupling of singlet and triplet states through the $K = 1/2$ bands. 3) Odd-odd nuclei have a "head-start" over other nuclei for producing high-spin and multi-particle states. However, very-heavy-ion beams become more important for studying these nuclei, since a large amount of angular momentum is "soaked up" in single-particle rather than collective motion.

We have begun a systematic study of neutron-deficient odd-odd Re nuclei with a ^{14}N beam on an ^{170}Er target. From excitation functions we have found the excitation energies needed to produce the different odd-odd Re

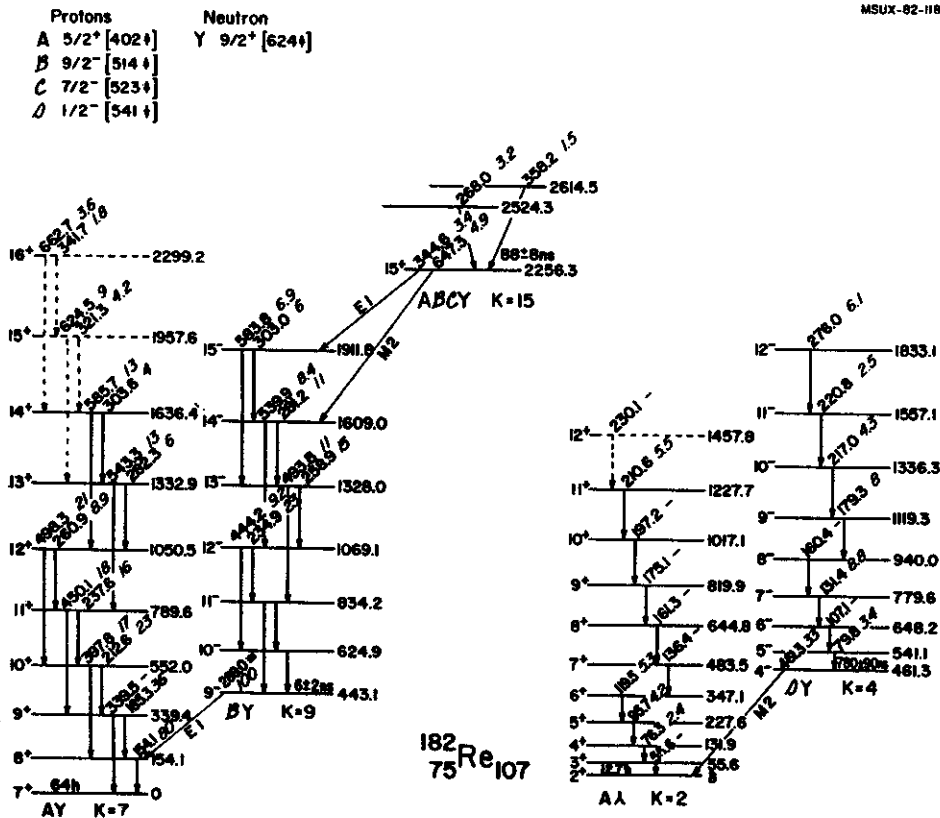


Fig. 1: ^{182}Re level scheme from Ref. [1]. All energies are given in keV, and γ -ray intensities are normalized to the 289.0 keV transition.

isotopes down through ^{172}Re , see Table 1. In

TABLE 1: REQUIRED EXCITATION ENERGIES

ISOTOPE	ENERGY
^{172}Re	9.18 MeV/n
^{174}Re	7.78 MeV/n
^{176}Re	5.43 MeV/n
^{178}Re	4.25 MeV/n
^{180}Re	3.13 MeV/n
^{182}Re	1.99 MeV/n

our first experiment, #84017 (in October-November 1984), we produced ^{182}Re and saw some indications of producing $^{180,178}\text{Re}$ (see Figure 2 which is a spectrum for ^{178}Re). Many of the bands seen in our gamma-ray spectra remain unidentified, but are in approximately the correct energy regions to indicate the presence of these Re isotopes. We are hoping to get more

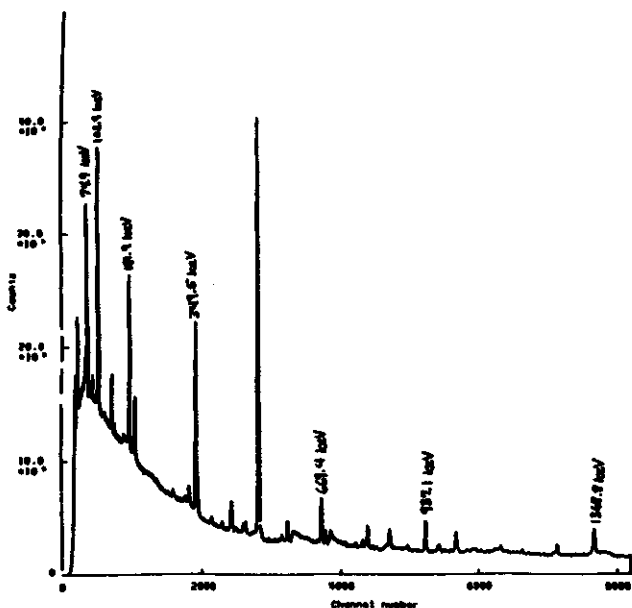


Fig. 2: A spectrum for ^{178}Re from our present work.

and better data in our next experiment, #85016, in order to be able to place the transitions

that we see into the bands of one of the odd-odd Re isotopes.

In future experiments we hope to use heavier beams i.e. ^{18}O and ^{22}Ne , in order to produce odd-odd Re isotopes which are excited into higher-angular-momentum states. This type of approach will give a more complete level scheme for these isotopes along with opening up the possibility of finding more states similar to the four-particle meta-stable state at 2256.3 keV identified in ^{182}Re [1]. This is depicted in Figure 3 and described as still basically

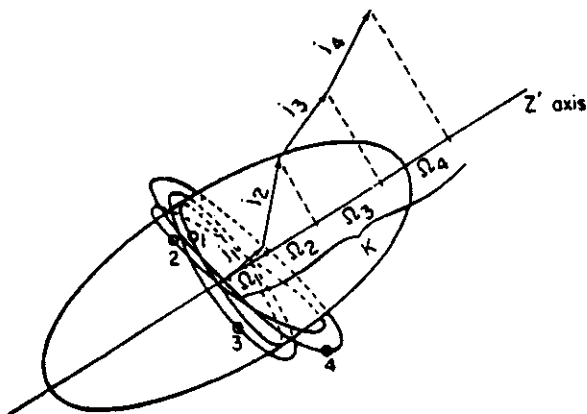


Fig. 3: Stylized sketch showing four high- Ω quasiparticles with their angular momenta uncoupled and aligned along the symmetry axis. These four nucleons provide an "effective" oblate girdle about a basically prolate core.

prolate, although the four particles produce an oblate "girdle" about the middle of the nucleus. A state such as this may indicate the beginning of a transition to "oblate-||" pseudo-rotational behavior. Thus, the study of the odd-odd deformed Re isotopes appears to have a rich and rewarding future.

1. M. F. Slaughter, R. A. Warner, T. L. Khoo, W. H. Kelly and Wm. C. McHarris, Phys. Rev. C29, 114(1984).

THE DECAY OF ^{223}Rn BY ^{14}C EMISSION

C.L. Tam, E. Kashy, D.J. Morrissey, S. Gales

The decay of ^{223}Rn by ^{14}C emission has been recently observed with a Si telescope¹, a solenoidal spectrometer² and with track detectors³. The branching ratio for this channel of decay has been reported to be extremely small: $((8.5 \pm 2.5) \times 10^{-10})^1$, $((5.5 \pm 2.0) \times 10^{-10})^2$ and $((6.1 \pm 1.0) \times 10^{-10})^3$, relative to α -decay. Calculations of the branching ratio for such a decay have also been published⁴. We have measured the decay with a different technique in a magnetic spectrograph.

A $n=1/2$, 30" radius magnetic spectrograph recently obtained from Argonne National Laboratory was used to study this decay channel. The solid angle was determined to be 15msr with a ^{228}Th source of known activity. The ^{223}Rn source used during the measurement had an activity of 0.45mCi which was measured with a Si detector in a well known geometry. The source was covered⁵ with a $30\mu\text{g}/\text{cm}^2$ layer of Au, and in addition, a $200\mu\text{g}/\text{cm}^2$ plastic foil was used during the experiment to prevent recoil nuclei from contaminating the spectrograph.

The carbon fragments were observed in two resistive-wire proportional counters at the focal plane. Both energy and position

information were obtained for each event. The magnetic field of the spectrograph was set to focus the expected 29.8MeV $^{14}\text{C}^{6+}$ ions on the detector. The $^4\text{He}^+$ ions having the same rigidity as the carbon ions were identified by their energy loss in the gas detector, which was no more than 2.22 Mev, while the ^{14}C energy loss was calculated to be about 7.5MeV.

A total of 104.5 hours was used for the measurement. Four events were observed in the detector with the energy loss expected for the ^{14}C 's and at the expected position on the focal plane. This yield corresponds to a branching ratio for ^{14}C emission relative to α -particles from ^{223}Rn of $(5.2 \pm 2.6) \times 10^{-10}$. The present measurement is thus in reasonable agreement with previous work and supports earlier reports using a different experimental method.

1. H. J. Rose and G. A. Jones, Nature (London) 307, 245 (1984)
2. S. Gales, E. Hourani, M. Hussonois, J. P. Schapira, L. Stab, and M. Vergnes, Phys. Rev. Lett. 53,759(1984).
3. P. B. Price, J. D. Stevenson and S. W. Barwick, Phys. Rev. Lett. 54,297(1984)
4. Yi-Jin Shi and W. J. Swiatecki, Phys. Rev. Lett. 54,300(1984)
5. Isotope Products Laboratories. 1800 No Keystone St. Burbsank, California 91504

ENERGY LEVELS OF ^{250}Bk Z. M. Koenig, Wm. C. McHarris and I. Ahmad^a

The odd-odd nucleus ^{250}Bk has been the subject of considerable interest in recent years, for its states can be probed in several different, complementary ways. It is the daughter of $276\text{-d } ^{254}\text{Es}^g$, a high-spin (7^+) nuclide whose α decay¹ populates a number of high-spin rotational bands in ^{250}Bk . The low-spin (2^+) isomer, $39.3\text{-h } ^{254}\text{Es}^m$, decays primarily by β^- emission to ^{254}Fm , but it has a 0.33% α -decay branch² that populates lower-spin rotational bands in ^{250}Bk . In addition, the recent availability of ^{249}Bk in large enough quantities for useful targets has made it feasible to perform transfer reactions such as $^{249}\text{Bk}(d,p)^{250}\text{Bk}$, which populates a more or less independent set of states in ^{250}Bk . Thus, for this particular heavy odd-odd nuclide we have a

relative wealth of varied experimental information, more, in fact, than is available for most lighter odd-odd nuclides.

Each of the three methods of populating the states of ^{250}Bk have been studied. The most recent one is the transfer reaction, $^{249}\text{Bk}(d,p)^{250}\text{Bk}$ by I. Ahmad which can now be added to the previous works and compared to nuclear Coriolis calculations.

a Chemistry Division, Argonne National Laboratory, Argonne, Ill.

References

1. Wm. C. McHarris, F. S. Stephens, F. Asaro, and I. Perlman, Phys. Rev. 144, 1031 (1966).
2. I. Ahmad, H. Diamond, J. Milsted, J. Lerner, and R. K. Sjoblom, Nucl. Phys. A208, 287 (1973).

